

Title No. 116-S56

A New Model for Crack Control in Reinforced Concrete Tank Walls—Part I: Analytical Investigation

by Mariusz Zych

A new calculation model for crack control in semi-massive reinforced concrete tanks used for liquid storage is proposed. The model includes three basic stages for the development of the crack width. The first stage covers the formation of early-age cracks occurring as a result of imposed loads acting during concrete hardening. The second stage concerns the formation of a stabilized spacing of basic cracks as well as the early period of imposed loads acting on a structure. The third stage involves sufficiently high values of imposed loads or, most frequently, service loads that result in the occurrence of second-order cracks and a simultaneous increase in the width of cracks formed in previous stages. In addition, instead of the degree of restraint, an average degree of relaxation was suggested as the basic parameter determining the crack width and spacing.

Keywords: codes of practice; crack control; early-age concrete; imposed deformation; reinforced concrete tank walls; semi-massive tanks; thermal stress.

INTRODUCTION

Some of the first experimental research on the cracking of base-restrained members was carried out by Stoffers.¹ It was demonstrated that cracking depends primarily on the degree of reinforcement and curvature of the element. The verification of standard formulas²⁻⁵ or approaches by various authors⁶⁻⁷ in comparison with the study of wall cracks on a natural scale, is extremely rare. As demonstrated by Zych,⁸ the models^{6,7} for certain cases are more accurate than those contained in EN 1992-3.⁴ Computational models predetermine a fixed crack spacing, as in the case of EN 1992-1-1,⁹ and EN 1992-3⁴ results from the model of a tie restrained at opposite ends and loaded with external forces. However, the crack spacing according to the Iványi⁶ and Rostásy and Henning⁷ models is equal to $(1/2)H$, which meets the condition of the minimum degree of reinforcement from Stoffers's¹ tests and is an arbitrary assumption for all computational cases.

Parametric analyses of the risk of cracking hardening concrete using advanced numerical models are presented in the following studies: Buffo-Lacarère et al.,¹⁰ Klemczak and Knoppik-Wróbel,¹¹ Liu et al.,¹² and Wu et al.¹³ In contrast, Kheder,¹⁴ Kheder et al.,¹⁵ and Al Rhawi and Kheder¹⁶ presented an analytical approach to determine the width of cracks in the walls restrained at the bottom edge while taking into account the pre- and post-cracking restraint coefficient; similar to the approach presented by Scott and Gill,¹⁷ they took into account the reduction in the crack width by reducing the imposed strain by $1/2\varepsilon_{ct}$. The current European standard dependencies (EN 1992-3⁴) regarding both cases of restraint—that is, along the bottom edge and the opposite

edges—were commented on by Beeby and Forth¹⁸ as well as by Beeby and Narayanan.¹⁹

Meanwhile, an analysis of the temperature field distribution and the resulting changes in the degree of restraint in base-restrained walls were presented by Anson and Rowlinson.^{20,21} It was demonstrated that the maximum degree of restraint did not occur at the bottom edge. Next, Pettersson and Thelander²² and Pettersson et al.²³ presented an analysis of walls restrained by foundation cracking while assuming a temperature change ΔT as a constant value in the section and in bilinear form. It was proven, most importantly, that the cracks first appeared at the level where the temperature profile changed along the height from linearly variable to uniform.

In practice, a continuous increment of the load over time results in an increase in both the width and the number of cracks. In the author's opinion, standard models—for example, in EN 1992-3,⁴ in which the stabilized spacing of cracks is predetermined at the concrete hardening stage (after thermal shrinkage only) and throughout the subsequent period of structure loading—are excessively simplified. In fact, the spacing of original cracks (that is, those that occurred from the low mechanical properties of concrete) is much larger. In contrast, the imposed loads generated by external restraints are too small (due to the concrete relaxation zones, Sections 2²⁴ and 4²⁴) to stabilize the crack spacing after only 5 days of concrete hardening. Therefore, in practice, the designer defines a standard crack spacing that is smaller than the actual one, thereby erroneously assuming effective crack propagation by reinforcement. Such an assumption is valid only for the tie model and the external loads from which the model originates. The thermal load during design is adopted as probable for actual thermal changes instead of a load that may result in the stabilized spacing of cracks. The effect of the aforementioned assumptions is a large underestimation of the calculated crack width. In other words, in the walls of reinforced concrete tanks cracked from imposed deformation, the crack spacing is both a function of the degree of external restraint, self-equilibrating stress, and the presence of reinforcement, the influence of which is not as dominant as in the case of tie models.

The only a general recommendation of allowing for the combined effect of imposed deformation and external loads

ACI Structural Journal, V. 116, No. 3, May 2019.

MS No. S-2018-140.R3, doi: 10.14359/51713317, received June 12, 2018, and reviewed under Institute publication policies. Copyright © 2019, American Concrete Institute. All rights reserved, including the making of copies unless permission is obtained from the copyright proprietors. Pertinent discussion including author's closure, if any, will be published ten months from this journal's date if the discussion is received within four months of the paper's print publication.

Title No. 116-S57

A New Model for Crack Control in Reinforced Concrete Tank Walls—Part II: Comparison with Experimental Results

by Mariusz Zych and Andrzej Seruga

This research paper demonstrates the use of a new crack control model, described in detail in PART I of the series, based on the results of in-place analyses of semi-massive reinforced concrete (RC) tank wall segments. The following results of the measurements are presented: changes in the temperature profile of the segment along its height and the imposed strains and changes in crack widths as a function of time. The calculations take into account the stages of the occurrence of imposed and external loads and the resulting changes in the crack widths. The results obtained are also presented with reference to the currently applicable provisions of the current European standard. In addition, the authors point to those elements of the model from EN 1992-3 that should be analyzed at this stage to make possible amendments to the guidelines of the standard.

Keywords: codes of practice; crack control; early-age concrete; imposed strains; reinforced concrete (RC) tank wall; semi-massive tanks, thermal stresses.

INTRODUCTION

In reinforced concrete (RC) tanks, cracks of excessive width cause leaks that prevent the proper use of the concrete tanks as well as the loss of durability and consequent loss of load-bearing capacity. This aspect frequently determines the degree of horizontal reinforcement in the walls. According to EN 1992-3¹ and other related standards (EN 1992-1-1,² EN 1990,³ EN 1991-1-1,⁴ EN 1991-1-3,⁵ EN 1991-1-5,⁶ EN 1991-4,⁷ EN 1997-1⁸), the crack criterion should be analyzed using various calculations resulting from the characteristics of a given tank.

Beeby⁹ was one of the first to introduce the mechanism of crack formation in the axially tension-loaded member. Concrete is most often assumed to be a linear-elastic and brittle material, as confirmed in studies by Scott and Gill¹⁰ and Beeby and Scott.¹¹

Another crack mechanism, mainly explaining large strains in sections between the cracks, was presented by Goto,¹² who also considered the possibility of the formation of internal cracks. This theory was developed using the finite element method (FEM), for example, by Forth and Beeby.¹³

The issues of interaction between the reinforcement and concrete around the crack as well as their impact on stiffness have been the subject of numerous studies, including, for example, Beeby and Scott,¹⁴ Beeby et al.,¹⁵ Clark and Cranston,¹⁶ Floegl and Mang,¹⁷ Whittle and Jones,¹⁸ Vollum,¹⁹ and Scott and Beeby.²⁰ The progressive loss of adhesion between steel and concrete, resulting from long-term loading as well as additional loads, causes decreased stiffness of the member and, in the case of imposed loads, also causes its relaxation.

In 1968, Evans and Hughes²¹ carried out one of the first studies on strain and temperature changes in an RC tank wall

with the degree of reinforcement of 0.57%. They demonstrated that greater efforts should be made to minimize temperature changes rather than shrinkage strains. They proposed a method for calculating the crack spacing in long walls restrained along the bottom edge using the following expression

$$\frac{f_{ct} \cdot \phi}{f_b \cdot 2 \cdot \rho} \geq S \geq \frac{f_{ct} \cdot \phi}{f_b \cdot 4 \cdot \rho} \quad (1)$$

They predetermined that, initially, the spacing of the cracks was twice as large until the next cracks appeared, while stresses in the concrete increased linearly from zero in a cracked cross section to the maximum value in the section distanced by s_{min} .

In 1970, Hughes and Miller²² were the first to measure the strain, temperature, and humidity of concrete as well as the strains of reinforcing steel on three RC walls in a natural scale constructed under various sets of ambient conditions. They exhibited good conformity with the expressions for crack spacing (Eq. (1)) and their widths.

In BS8007,²³ the method of calculating the crack width was, to a certain extent, very similar to the current provisions of EN 1991-1-3.¹ The width of the crack was calculated from the formula shown as follows

$$w_{max} = s_{max} \cdot \varepsilon \quad (2)$$

where the spacing of the cracks was defined as in the model developed by Evans and Hughes²¹

$$s_{max} = (f_{ct}/f_b) \cdot \phi/2\rho \quad (3)$$

whereas the strain could be determined as

$$\varepsilon = [(\varepsilon_{cs} + \varepsilon_{te}) - 100 \times 10^{-6}] \text{ or } \varepsilon = R \cdot \alpha_T \cdot \Delta T \quad (4)$$

Al-Rawi and Kheder,²⁴ when modifying Eq. (3) for the spacing of cracks included in BS8007,²³ predetermined that in the walls restrained at the base, the spacing of cracks depended both on the strength of reinforcement and the degree of restraint along the bottom edge. Thus, the expression for crack spacing took into account the height of the wall

ACI Structural Journal, V. 116, No. 3, May 2019.

MS No. S-2018-141.R1, doi: 10.14359/51713318, received May 23, 2018, and reviewed under Institute publication policies. Copyright © 2019, American Concrete Institute. All rights reserved, including the making of copies unless permission is obtained from the copyright proprietors. Pertinent discussion including author's closure, if any, will be published ten months from this journal's date if the discussion is received within four months of the paper's print publication.

$$s_{min} = \frac{k \cdot \phi \cdot H}{\rho \cdot H + k \cdot \phi} \text{ and } s_{max} = 2s_{min} \quad (5)$$

where $k = f_i/(4f_b) = 0.57, 0.68,$ and 0.85 for deformed, indented, and plain reinforcement, respectively.

Kheder and Fadhil²⁵ continued the approach of Al-Ravi and Kheder,²⁴ and they took into account the effect of elastic shrinkage of the foundation with the K factor, according to ACI.²⁶ Then, they modified the expression for the maximum crack width contained in BS8007.²³ Finally, they obtained an expression that depended on the degree of restraint and elastic shrinkage of the foundation

$$w_{max} = 0.5s_{max} \cdot (0.5KR \cdot (\epsilon_{th} + \epsilon_{sh}) - \epsilon_{ctu}) \quad (6)$$

Equation (6) was very similar to Harrison's²⁷ proposal

$$w_{max} = s_{max} \cdot (0.5R_b \cdot (\epsilon_{th} + \epsilon_{sh}) - \epsilon_{ult}/2) \quad (7)$$

which was a modification of the expression contained in BS 5337²⁸

$$w_{max} = s_{max} \cdot (0.5\epsilon_{th} + \epsilon_{sh} - \epsilon_{ult}/2) \quad (8)$$

The expressions for calculating the crack width were evolving. However, a major amendment was presented by Harrison²⁷ (Eq. (8)). This amendment introduced the coefficient of the degree of external restraint, which allowed the prediction of the change in the crack width along the height of the wall, while in BS 5337,²⁸ a constant crack width was defined. In addition, in BS 5337,²⁸ as in BS 8007,²³ concrete creep was included in a 50% reduction of the restrained part of thermal strains.

Kheder and Fadhil²⁵ claimed that limited widths of cracks in the walls restrained along the bottom edges result both from reinforcement and restraint at their bases. Therefore, less reinforcement could be used than in the members restrained at opposite ends only. In addition, they stated that to use more economical solutions, the degree of reinforcement should depend on the changing degree of restraint of the wall. In the next study, Kheder et al.²⁹ defined the formula for the crack width in the following form

$$w_{max} = s_{max} \cdot [C_1(R_b - C_2R_a) \cdot \epsilon_{free} - \epsilon_{ctu}/2] \quad (9)$$

where R_b is the coefficient of restraint before cracking in the middle of the wall length; and R_a is the coefficient of restraint after cracking on the wall edge (defined using FEM for the segment with a L/H ratio that is two times smaller and without reinforcement).

Due to the important role of the restraint coefficient, Klemczak and Knoppik-Wróbel³⁰ demonstrated the significant influence of support conditions on its value. They demonstrated that if the possibility of wall rotation was considered, the degree of restraint in the structural joint increased, whereas it decreased in the upper part of the wall. This influence is more noticeable for longer walls and is almost unnoticeable in the case of shorter walls.

According to the authors, there is a need to create a model that can combine the specific behavior of the shells of RC tanks, especially under the influence of imposed loads, both in the case of segments restrained at the base and along three edges, including the possible increase in the crack width under the influence of the value and type of loads (imposed and external). This conclusion is confirmed by the research on the manner of cracking of the walls of RC tanks presented in the research paper,³¹ which demonstrated a different characteristic than was assumed in tie models. The only general recommendation of allowing for the combined effect of imposed deformation and external loads on the crack width calculation was introduced with certain restrictions in DIN EN 1992-1-1/NA.³² This approach is fully based on equations defined in EN 1992-1-1.²

RESEARCH SIGNIFICANCE

The results of in-place studies of a semi-massive segment of the RC tank wall provide information about the development of cracks over time as the imposed load changes. The research also provided the basis for the verification of a new crack control model, which considers the influence of the staging of imposed loads on changes in the crack width, which is an issue that was previously unrecognized in the world literature or current standards. The results can serve as a basis of future code changes for crack control coming from hydration temperature, elevated temperature, shrinkage, and external load effects.

EXPERIMENTAL INVESTIGATION

Results of in-place research studies

The subject of this research is the wall segment restrained along three edges with dimensions of $L/H/h = 15.7 \text{ m}/6.4 \text{ m}/0.6 \text{ m}$ (51.5 ft/21 ft/2 ft), described in detail in the research paper.³¹ Figure 1 illustrates a simplified distribution of the cracks that were formed before Day 16 after the concreting of the wall, which resulted from the early-age imposed loads. Considering the early age of hardening of the concrete, the concrete shows numerous cracks, which were caused by a very high degree of reinforcement. Figure A-1* illustrates a further stage of the cracking, just before the water-tightness test—3 months after the concreting of the wall. When compared to the layout of the cracks from Day 16, the wall is characterized by a significant increase in the crack length and the formation of new cracks, reducing the average spacing from 0.24 m (0.79 ft) to 0.20 m (0.66 ft). Such heavy cracking was caused by imposed loads only. The last of the presented stages of the cracking is 9.5 months after the concreting of the segment, which includes a tank water-tightness test carried out in the winter period (water was not allowed to freeze [Fig. A-2]). Compared to the layout of the cracks before the water-tightness test, a small number of newly formed cracks and the occasional extension of the cracks toward the bottom edge of the wall were observed. In the first stage (Fig. 1), the crack width measured

*The Appendix is available at www.concrete.org/publications in PDF format, appended to the online version of the published paper. It is also available in hard copy from ACI headquarters for a fee equal to the cost of reproduction plus handling at the time of the request.

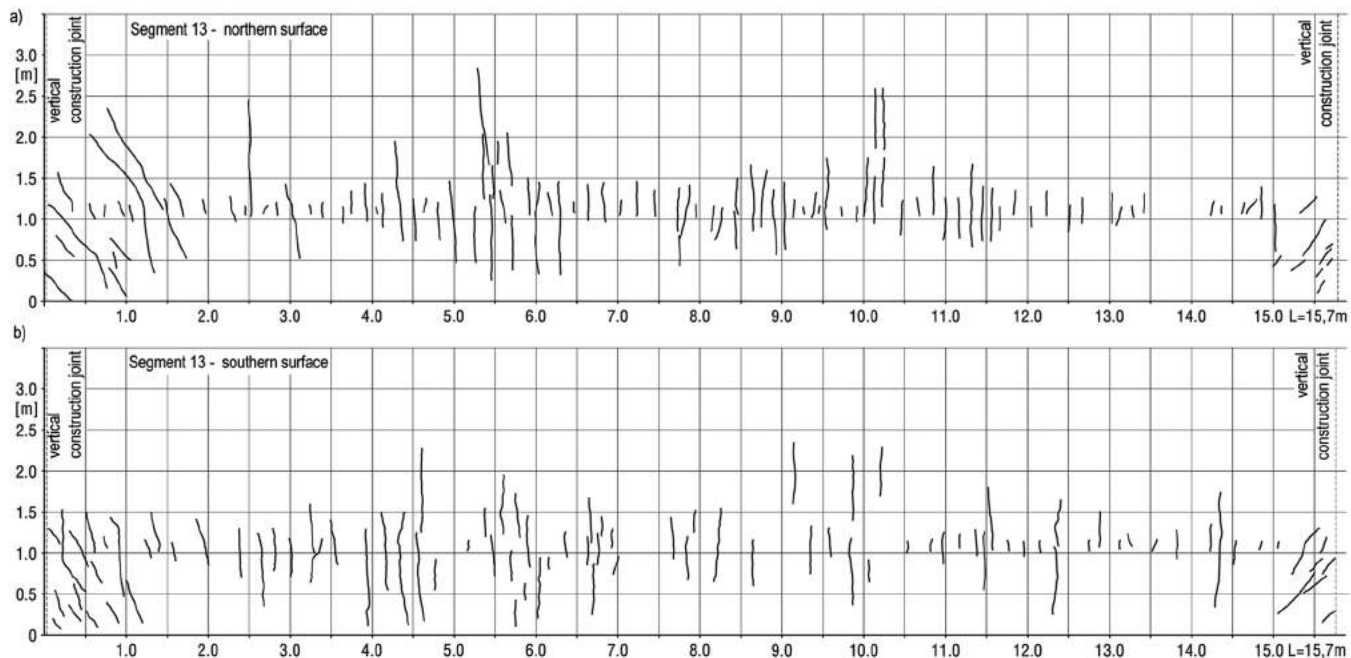


Fig. 1—Layout of cracks formed over period of 16 days after concreting on segment 13: (a) on north side; and (b) on south side. (Note: 1 m = 3.28 ft.)

with the Brinell’s magnifying glass did not exceed 0.1 mm (3.9 mil) and, in most cases, the cracks were limited to 0.075 mm (2.9 mil) (compare detailed Fig. 7³³). In the second stage (Fig. A-1), the crack width measured only occasionally and locally (that is, on very short sections of the cracks) reached the values of 0.15 mm (5.9 mil), and in the remaining cases they were limited to 0.1 mm (3.9 mil). During the last measurement stage (Fig. A-2), the cracks did not widen.

The concrete was poured on a hot day, so the initial temperature of the concrete soared up to 29.0°C (84.2°F). The increasing hydration heat contributed to the wall’s maximum temperature of 45°C (113°F), measured at the height of 2.5 m (8.2 ft) from its base. The formwork was removed from the southern surface after 20 hours of concrete maturing, which prevented further increase of concrete temperature. In case of the northern surface, the formwork was removed after 40 hours of concrete maturing. Specific changes of temperature during concrete maturing, in the wall’s cross section, were presented by Seruga and Zych.³³ As seen in Fig. 2, the differences in temperature of the concrete in the middle part of the wall, determined in relation to its maximum value, in the subsequent stages were as follows:

- $\Delta T_m = 17.1^\circ\text{C}$ (30.8°F) on 28-08, 10:30 (2.6 days after concreting),
- $\Delta T_m = 29.6^\circ\text{C}$ (53.3°F) on 31-08, 10:00 (5.6 days after concreting),
- $\Delta T_m = 39.5^\circ\text{C}$ (71.1°F) on 21-09, 7:30 (26.5 days after concreting),
- $\Delta T_m = 41.4^\circ\text{C}$ (74.5°F) on 26-10, 10:00 (61.6 days after concreting),
- $\Delta T_m = 49.0^\circ\text{C}$ (88.2°F) on 24-11, 11:00 (90.6 days after concreting).

Because the strength of the concrete in the cross section at the wall thickness is also determined by the temperature difference there, Fig. 3 illustrates those differences

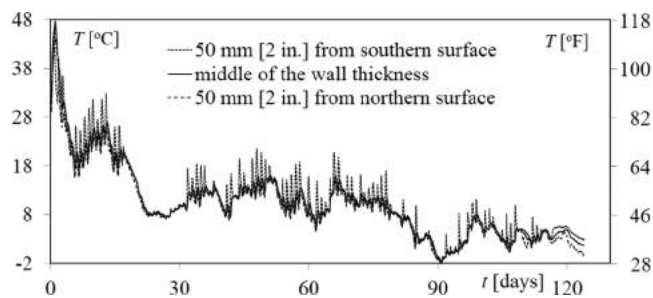


Fig. 2—Measured temperature changes inside wall and at of outer layer of horizontal main reinforcement (at north and south surfaces of wall). (Note: 1°F = 1.8°C + 32.)

(ΔT_h) between the temperatures measured at points located at different distances from the surface of the wall and the temperature measured in the middle of the wall thickness. The sensors were placed at the height of 2.5 m (8.2 ft) from the base of the added segment. Figures 3(a) and (b) relate to the points located in the wall halves located on the south and north sides, respectively. The differences in the values obtained for the southern and northern parts of the wall are essential and are directly related to the varied solar radiation on both surfaces. The short measurement period presented, from the moment of concreting to Day 16, results from the repetitious values of ΔT_h later on. The values are smaller in the winter. At a characteristic point of time, the temperature differences between the inside of the wall and the northern wall surface (ΔT_{pn}) and the southern wall surface (ΔT_{pd}) are as follows:

- $t = 1.1$ days, $\Delta T_{pn} = -4.5^\circ\text{C}$ (-8.1°F), $\Delta T_{pd} = -14.5^\circ\text{C}$ (-26.1°F),
- $t = 2.2$ days, $\Delta T_{pn} = -7.8^\circ\text{C}$ (-14.0 °F), $\Delta T_{pd} = -8.2^\circ\text{C}$ (-14.8°F),
- $t = 2.7$ days, $\Delta T_{pn} = -3.1^\circ\text{C}$ (-5.6°F), $\Delta T_{pd} = +8.4^\circ\text{C}$ (+15.1°F),

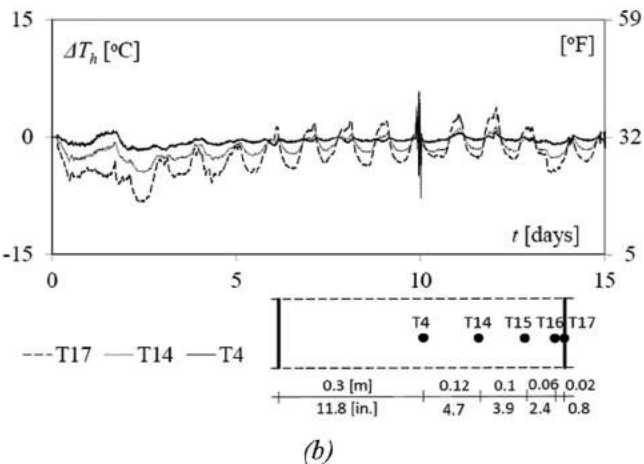
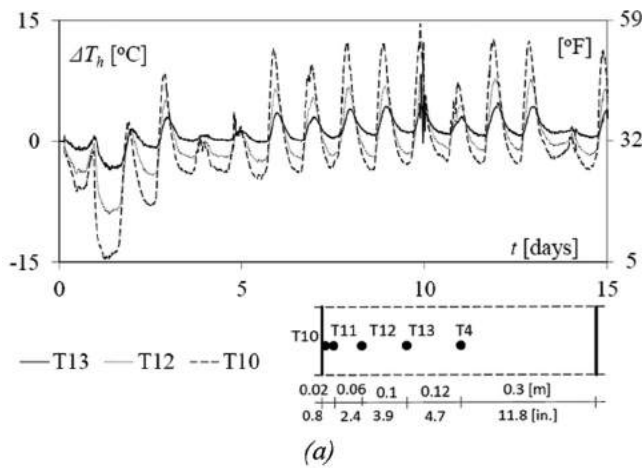


Fig. 3—Measured temperature differences between points distributed over wall thickness and interior of wall: (a) for points located on southern side; and (b) for points located on northern side. (Note: $1^{\circ}\text{F} = 1.8^{\circ}\text{C} + 32$.)

- $t = 5.2$ days, $\Delta T_{pn} = -4.6^{\circ}\text{C}$ (-8.3°F), $\Delta T_{pd} = -4.6^{\circ}\text{C}$ (-8.3°F),
- $t = 5.7$ days, $\Delta T_{pn} = -0.6^{\circ}\text{C}$ (-1.1°F), $\Delta T_{pd} = +11.5^{\circ}\text{C}$ ($+20.7^{\circ}\text{F}$),
- $t = 7.7$ days, $\Delta T_{pn} = +1.0^{\circ}\text{C}$ ($+1.8^{\circ}\text{F}$), $\Delta T_{pd} = +12.2^{\circ}\text{C}$ ($+22.0^{\circ}\text{F}$).

Negative values mean a lower temperature at the wall surface than inside the wall. Such a case is dominant in the early stage of concrete hardening and means that additional tensile stresses occur at the surface of the wall in relation to the tensile stresses resulting from changes in the average temperature and degree of external restraint. From a practical point of view, one can conclude that the temperature differences later do not exceed $\pm 5^{\circ}\text{C}$ (9°F), except for the surface of the wall subjected to intense solar radiation, which results in the reduction of tensile stresses on the sunlit surface and the increase in tensile stress on the shaded surface of the wall. However, at the time when the southern surface is shaded, it is cooled down even by 15°C (27°F) in a very short time.

Figure 4 illustrates the measured changes in concrete strains, constituting an unrestricted part of the imposed strains. In the early period, when the temperature rises, a

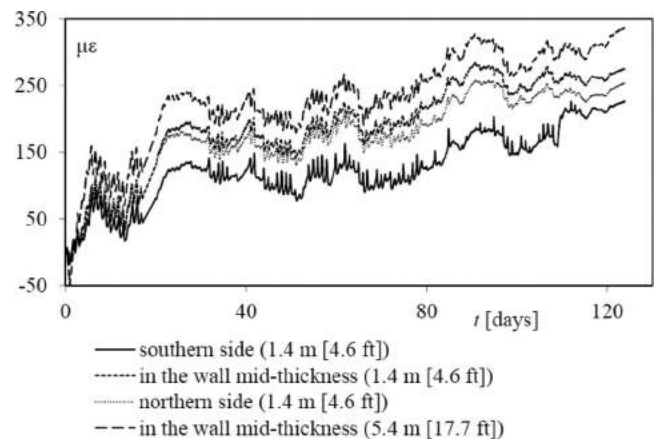


Fig. 4—Changes in free strain measured in concrete.

small swelling of concrete, up to $50 \mu\epsilon$ at the measured height of 5.4 m (17.7 ft) and $19 \mu\epsilon$ at the measuring height of 1.4 m (4.6 ft), is observed. The temperature drop inside the wall of $\Delta T_m = 29.6^{\circ}\text{C}$ (53.3°F) occurs up to 5.6 days after concreting and contributes to the formation of strains of the opposite sign, with the values of ~ 158 and $115 \mu\epsilon$, respectively. After 3 months, when $\Delta T_m = 49.0^{\circ}\text{C}$ (88.2°F), these strains are ~ 340 and $250 \mu\epsilon$, respectively. The results presented in Fig. 2 and 4 define the value and constant increase in the imposed load, which may suggest continuous changes in the widths and number of cracks.

However, Fig. 5(a) and (b) demonstrate the measured changes in the widths of selected cracks on the north and south sides of the wall segment, respectively. The diagrams were prepared based on the measurements of the strains carried out with the Demec sensor on a 100 mm (3.9 in.) measuring stand (in the same way as illustrated in Fig. 5³⁴ and 6³⁴). The results of the measurements of the strains along the entire length of the segment on its northern and southern sides are illustrated in Fig. 4.³³ The descriptions in the legends to Fig. 5(a) and (b) refer to the location of the cracks along the length of the segment (compare with Fig. 1).

Figure 6 presents the measured mean value of shrinkage. The dashed lines represent the results of the calculations of total shrinkage according to EN 1991-1-1² made for the analyzed samples for the relative humidity $\text{RH} = 50$ and 80% . Starting from Day 22, the measurement results fall within the range of values calculated in accordance with EN 1991-1-1.²

An important role in the calculation of stresses and widths of cracks is played by the mechanical properties of concrete and, in particular, the changes in these mechanical properties over time in the period of intense temperature changes mainly originating from the development of the heat of hydration. In this case, concrete with C30/37 strength class was used on CEM III/A 32.5N cement. The average tensile strengths of 0.736 , 0.921 , 1.1025 , 1.256 , 1.437 , 1.71 , 1.839 , and 1.987 MPa (0.11 , 0.13 , 0.16 , 0.18 , 0.21 , 0.25 , 0.27 , and 0.29 ksi), respectively, were obtained from the axial tensile strength tests carried out on $\phi 150 \times 300 \text{ mm}$ ($\phi 5.9 \times 11.8 \text{ in.}$) samples at $t = 1.5, 2, 4, 5, 7, 28, 60$, and 90 days, respectively. The results of concrete modulus of elasticity tests carried out on $\phi 150 \times 300 \text{ mm}$ samples are presented in Fig. 7. It was

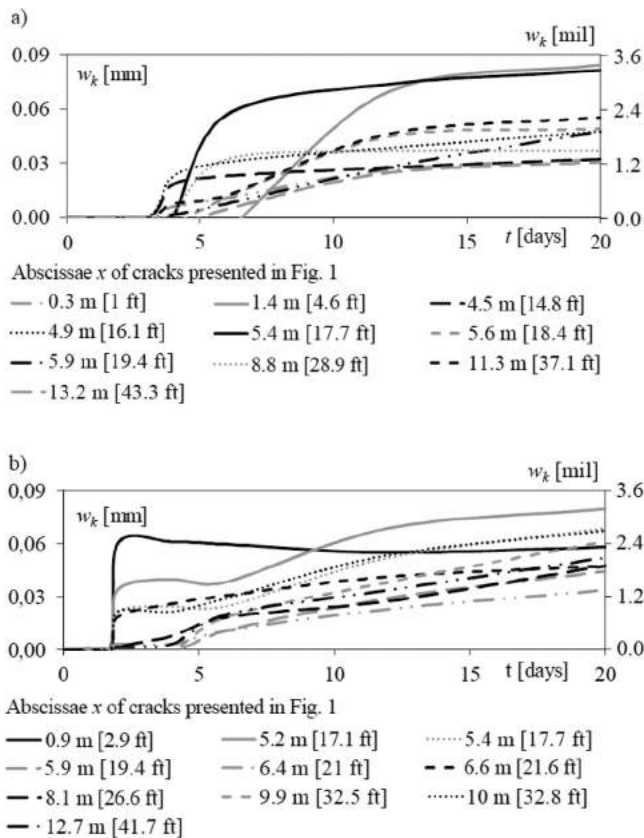


Fig. 5—Measured changes in widths of selected cracks over time, located in Fig. 1 according to abscissae x , determined based on measured strains as illustrated in Fig. 4³³: (a) on north side; and (b) on south side of wall segment. (Note: 1 m = 3.28 ft; 1 mm = 0.0394 in.)

necessary to calibrate the basic function (Eq. (3.2)²) in which the coefficient s played an essential role in the increment rate of the mechanical properties of concrete. According to EN 1991-1-1,² for the cement used in CEM III/A 32.5 N, the value of s is equal to 0.38. The obtained development of the modulus of elasticity for this value of the coefficient is illustrated with a continuous line in Fig. 7. In comparison to the examined values, a significant overestimation of the development rate of the modulus of elasticity was observed at the early age of concrete curing, as was the underestimation of the rate for $t = 90$ days. The conducted calibration of the coefficient s up to the value of 0.79 allowed a satisfactory consistency with the test results to be obtained, as illustrated by the dashed line.

COMPARISON OF PREDICTIONS AND EXPERIMENTAL RESULTS

Mechanical properties of concrete

When the increase in mechanical properties of concrete over time was being determined, the thermal conditions under which concrete was hardening were considered. When the increase in tensile strength and secant modulus of elasticity of concrete over time were being determined, the thermal conditions under which concrete was hardening were considered.

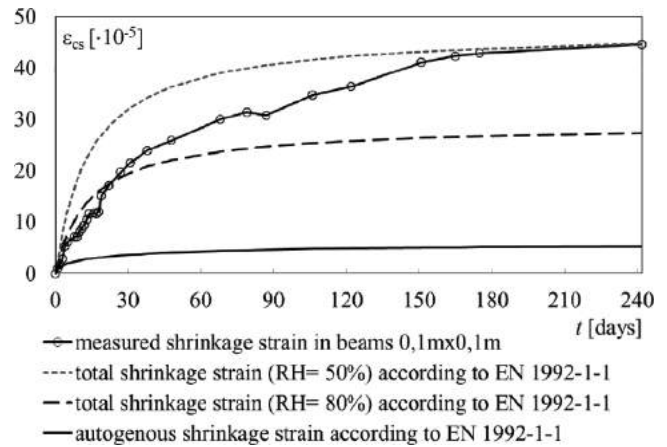


Fig. 6—Measured and calculated shrinkage of C30/37 concrete.

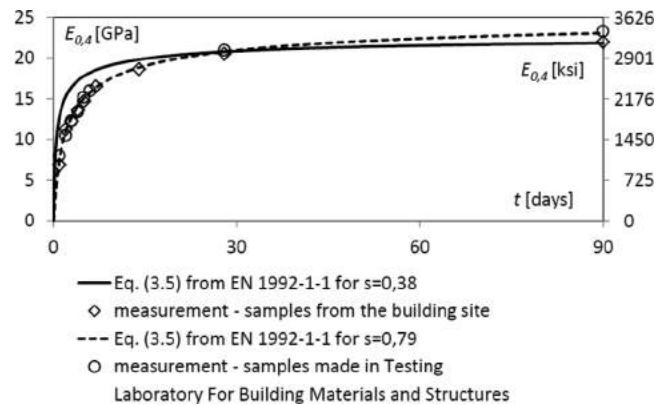


Fig. 7—Measured and calculated development of modulus of concrete elasticity. (Note: 1 GPa = 145 ksi.)

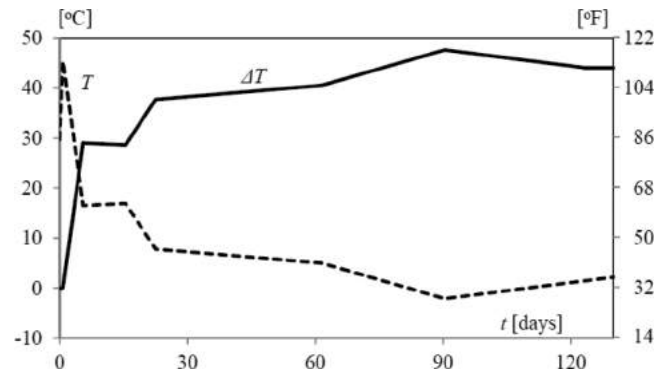


Fig. 8—Change in average temperature (T) of wall and temperature difference (ΔT). (Note: $1^{\circ}\text{F} = 1.8^{\circ}\text{C} + 32$.)

For this purpose, the dependencies B.10,² 3.2,² 3.4,² 3.5² contained in EN 1992-1-1² were used. Based on the course of the average temperature of the wall over time, an increase in the temperature difference was obtained (ΔT measured from the maximum temperature T_{max} [Fig. 8]).

Crack criterion

The adopted height $h_1 = 1.15$ m (3.8 ft) results from the observation of the point of crack initiation for this segment (Fig. 1) and from the measurement of temperature changes at the height of this segment (compare with Fig. 2³⁵). Hence,

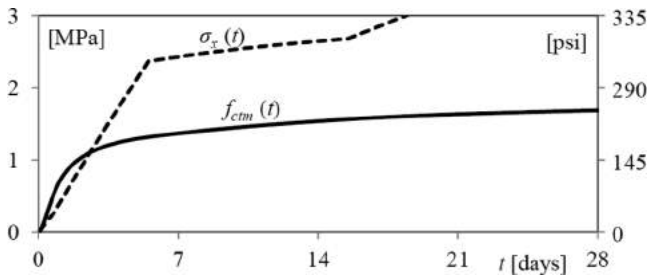


Fig. 9—Increase in thermal stresses and tensile strength. (Note: 1 MPa = 145 psi.)

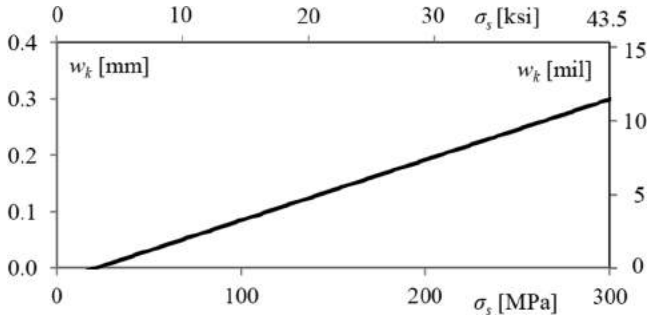


Fig. 10—Width of crack as function of stresses in reinforcing steel. (Note: 1 MPa = 145 psi; 1 mm = 0.0394 in.)

$h_1/H = 1.15 \text{ m}/6.4 \text{ m} = 0.18$. Then, the coefficient of the external degree of restraint in the critical cross section was determined, which has a characteristic value of $h_1/H = 0.18$ (Table 1³⁵), and interpolating for $L/H = 2.45$ and $\alpha_D = 1.98/\text{m}$ (0.6/ft) (α_D – value obtained from the expression $\alpha_D = D_{11}/E_{cm}$), having determined $k_r(\sigma_s)$ according to Eq. (14)), $R_{ax}^{uc}(0.5L) = 0.979$ was obtained. Tensile stresses were determined using Eq. (10), taking into account the influence of compressive stresses in the form of the coefficient k_σ and the influence of creep by the coefficient k_ϕ and the influence of self-equilibrating stresses resulting from non-uniform temperature distribution. In general, self-equilibrating stresses may lead to an increase of tensile stresses not only at the element's surface but also inside it. This depends on when the formwork is removed, which causes a different temperature distribution in the wall's cross section.³⁶

$$\sigma_x(t) = (1 - k_\sigma)k_\phi R_{ax}^{uc} \alpha_c \Delta T(t) E_{cm}(t) + k_\phi R_{ax}^{uc} \varepsilon_{ca}(t) E_{cm}(t) + \alpha_c \Delta T_h(t) R_h E_{cm}(t) \quad (10)$$

where $k_\phi = 0.65$; $\alpha_T = 0.00001/^\circ\text{C}$ (0.0000056/ $^\circ\text{F}$); $\Delta T(t)$ is defined as in Fig. 8; k_σ is 0.46 (value determined based on previous studies [compare Fig. 11³⁷]); $\varepsilon_{ca}(t)$ is autogenous shrinkage determined based on the relationships contained in EN 1992-1-1² (refer to Fig. 6); $\Delta T_h = 5^\circ\text{C}$ (9 $^\circ\text{F}$); and $R_h = 0.36$. Coefficient $k_\phi = 0.65$ used in Eq. (10) was adopted following the CIRIA C660³⁸ recommendations. It should be emphasized that it is a simplifying assumption since CIRIA C660,³⁸ general recommendations do not take account of the cement kind on the concrete creep extent.

Stress changes $\sigma_x(t)$ and increases in the average tensile strength of concrete for calibrated value of $s = 0.79$ are

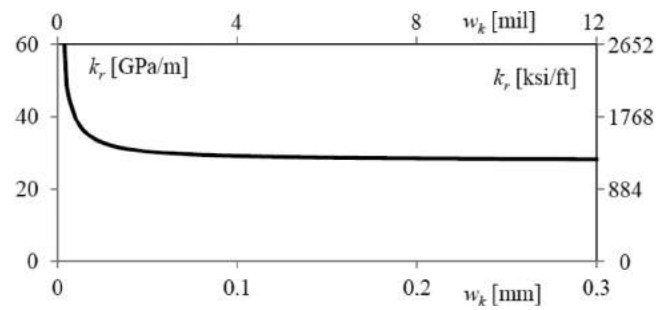


Fig. 11—Distributed elastic stiffness from reinforcement in entire cross section of crack as function of its width. (Note: 1 GPa/m = 44.2 ksi/ft; 1 mm = 0.0394 in.)

illustrated in Fig. 9. The first surface cracks will be formed on the third day after the concreting of the wall segment, precisely for $t_{cr} = 2.6$ days. The trough cracks (which neglect self-equilibrating stresses) will form 3.5 days after the concreting of the wall segment—that is, the trough cracks could be observed on the fourth day after the concreting of the wall.

Stiffness of discrete crack

The effective depth of the cross section is $d = h - c_{nom} - \phi_{20} - \phi_{20}/2 = 600 \text{ mm} - 40 \text{ mm} - 3/2 \cdot 20 \text{ mm} = 530 \text{ mm}$ (1.74 ft). According to EN 1992-1-1,² the effective reinforcement ratio is $\rho_{p,eff} = 0.5A_s/A_{ceff} = 0.5 \cdot 104.3 \text{ cm}^2/[1 \text{ m} \cdot (2.5(600 \text{ mm} - 530 \text{ mm}))] = 2.98\%$. The length of the relaxation zone, according to Eq. (3),³⁵ is: $s_{ro} = c_{nom} + k_1 \cdot k_2 \cdot k_4 \cdot \phi/\rho_{p,eff} = 40 \text{ mm} + 0.125 \cdot 0.8 \cdot 1.0 \cdot 20 \text{ mm}/2.98\% = 107 \text{ mm}$ (4.2 in.).

Figure 10 illustrates the crack width at the surface of the wall as a function of stresses in steel, according to Eq. (11)

$$\begin{aligned} w_k(\sigma_s) &= \frac{\sigma_s}{E_s} \cdot 2 \cdot s_{ro} - \frac{k_i \cdot f_{ct,eff}(t_{cr})}{E_s \cdot \rho_{p,eff}} \cdot 2 \cdot s_{ro} - \frac{k_i \cdot f_{ct,eff}(t_{cr})}{E_{cm}(t_{cr})} \cdot 2 \cdot s_{ro} \\ &= \frac{\sigma_s}{200 \text{ GPa}} \cdot 2 \cdot 0.107 \text{ m} - \frac{0.4 \cdot 1.11 \text{ MPa}}{200 \text{ GPa} \cdot 2.98\%} \cdot 2 \cdot 0.107 \text{ m} \\ &\quad - \frac{0.4 \cdot 1.11 \text{ MPa}}{15.8 \text{ GPa}} \cdot 2 \cdot 0.107 \text{ m} = 1.071 \sigma_s \text{ mm/GPa} - 0.022 \text{ mm} \\ &= 0.291 \sigma_s \text{ mil/ksi} - 0.866 \text{ mil} \end{aligned} \quad (11)$$

A significant change in the crack width mainly results from the low mechanical properties of concrete and taking into account two full-length relaxation zones s_{ro} . The next step involves the determination of adhesion stress

$$f_{bk} = 2.25 \cdot \eta_1 \cdot \eta_2 \cdot f_{ctk}' = 2.25 \cdot 0.7 \cdot 1.0 \cdot (0.7 \cdot 1.11 \text{ MPa}) = 1.22 \text{ MPa} (177 \text{ psi}) \quad (12)$$

Thus, the distributed stiffness between bond and slip along the reinforcement bar is

$$\begin{aligned} k_b(\sigma_s) &= \frac{f_{bk}}{w_k(\sigma_s)} = \frac{1.22 \text{ MPa}}{1.071 \sigma_s \text{ mm/GPa} - 0.022 \text{ mm}} \\ &= \frac{0.177 \text{ ksi}}{0.291 \sigma_s \text{ mil/ksi} - 0.866 \text{ mil}} \end{aligned} \quad (13)$$

As presented by Pettersson and Thelandersson,³⁹ the general solution for the displacement of the bar $u(x)$ supported by springs arranged along its axis was first proposed by Volkersen.⁴⁰ Using this approach, a distributed elastic stiffness from reinforcement k_r was obtained for the entire cross-section of the crack (Eq. (14)). The change in stiffness k_r as a function of the crack width is demonstrated in Fig. 11.

$$k_r(\sigma_s) = \frac{\sqrt{\frac{k_b(\sigma_s) \cdot E_s}{\phi}} \cdot \rho_{p,eff}}{\tanh(\lambda a)}$$

$$= \frac{\sqrt{\frac{1.22 \text{ MPa}}{1.071 \sigma_s \text{ mm/GPa} - 0.022 \text{ mm}} \cdot 200 \text{ GPa}}}{\tanh(\lambda(\sigma_s) \cdot 0.107 \text{ m})} \cdot 2.98\%$$
(14)

where

$$\lambda(\sigma_s) = \sqrt{\frac{k_b(\sigma_s) \cdot \pi \cdot \phi}{E_s \cdot A_\phi}}$$

$$= \sqrt{\frac{1.22 \text{ MPa}}{1.071 \sigma_s \text{ mm/GPa} - 0.022 \text{ mm}} \cdot 3.14 \cdot 20 \text{ mm}}}{200 \text{ GPa} \cdot 3.14 \text{ cm}^2}$$
(15)

For further calculations, $D_{11} = k_r(w_k = 0.03 \text{ mm [1.2 mil]}) = 31.4 \text{ GPa/m (1388 ksi/ft)}$; hence, $\alpha_D = D_{11}/E_{cm}(t_{cr} = 2.6 \text{ days}) = 31.4 \text{ GPa}/15.8 \text{ GPa} = 1.98/\text{m (0.6/ft)}$ was adopted.

Spacing of first-order cracks

The average effective degree of wall relaxation (Table 1 of Part 1 of this study³⁴) after the interpolation for $h_1/H = 0.18$ and $\alpha_D = 1.98/\text{m (0.6/ft)}$ is $\Delta R_{ax}(0.25L/L; 0.75L/L) = 0.0239$. According to Eq. (17),³⁴ a stabilized spacing of the first-order cracks was obtained: $s_{rml} = 2H \cdot 0.0239/0.3855 = 0.79 \text{ m (2.59 ft)}$.

The coefficient of restraint in the cross-section distance from the cracked critical cross-section s_{rml} is a function of h_1/H and α_D (Fig. 4(a)⁴¹; Table 1⁴¹). The variable $x = 0.015$ results from the product $(s_{rml}/2.45H) \cdot (2.45/8)$. The first component of the product defines the relative distance from the crack to the place where the next crack may be formed. The second component is the rescaling of variable x on graph 12 due to the length of the wall smaller than $8H$. $R_{ax}^c(s_{rml}) = R_{ax}^{uc}(0.5L) - \Delta R_{ax}((s_{rml}/2.45H) \cdot (2.45/8); (\alpha_D = 1.98/\text{m}))$.

According to the following expression

$$R_{ax}(x, \alpha_D) = y_o + a \cdot \exp\left(-\exp\left(\frac{-(x-x_o)}{b_o}\right)\right) - \left(R_{ax}^{uc}\left(\frac{L}{H} = 8\right) - R_{ax}^{uc}\left(\frac{L}{H} = 2.45\right)\right)$$
(16)

and the coefficients from Table 2³⁵: for $\alpha_D = 1.0 \rightarrow a(1.0) = 0.1633$, $b(1.0) = 0.0200$, $x_o(1.0) = 0.0235$, $y_o(1.0) = 0.8116$, for $\alpha_D = 2.5 \rightarrow a(2.5) = 0.0662$, $b(2.5) = 0.0173$,

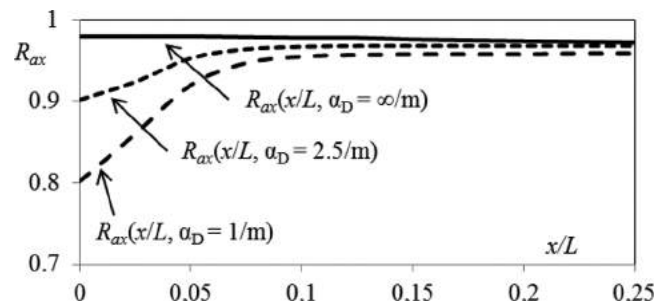


Fig. 12—Changes in degree of restraint around crack along length of wall with L/H ratio of 2.45. (Note: $1/\text{m} = 0.305/\text{ft}$.)

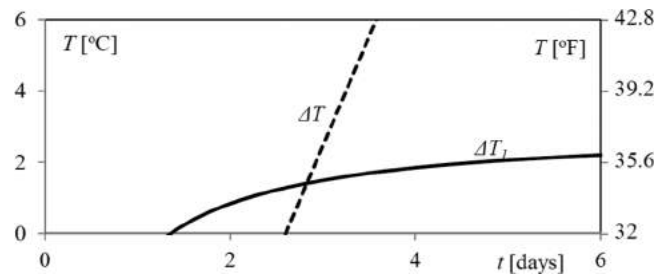


Fig. 13—Changes in permissible (ΔT_1) and real (ΔT) temperature. (Note: $1^\circ\text{F} = 1.8^\circ\text{C} + 32$.)

$x_o(2.5) = 0.0264$, $y_o(2.5) = 0.9182$, the changes in the degree of restraint were obtained around the crack (Fig. 12).

The effective degree of relaxation in the section spaced by s_{rml}

$$\begin{aligned} & \Delta R_{ax}((s_{rml}/2.45H) \cdot (2.45/8); (\alpha_D = 1.98/\text{m})) \\ &= \Delta R_{ax}((s_{rml}/2.45H) \cdot (2.45/8); (\alpha_D = \infty/\text{m})) \\ & \quad - \{ \Delta R_{ax}((s_{rml}/2.45H) \cdot (2.45/8); \\ & \quad \alpha_D = 1.0) + [\Delta R_{ax}((s_{rml}/2.45H) \cdot (2.45/8); \alpha_D = 2.5) \\ & \quad - \Delta R_{ax}((s_{rml}/2.45H) \cdot 2.45/8; \alpha_D = 1.0)] (1.98/\text{m} - \\ & \quad 1.0/\text{m}) / 1.5/\text{m} \} = 0.979 - [0.831 + (0.911 - 0.831) \\ & \quad (1.98/\text{m} - 1.0/\text{m}) / 1.5/\text{m}] = 0.096. \end{aligned}$$

Hence, $R_{ax}^c(s_{rml}) = 0.979 - 0.096 = 0.883$.

Figure 13 illustrates the actual change in the temperature difference ΔT and the values of ΔT_1 calculated in accordance with Eq. (17). The figure demonstrates that in the time of $t_1 = 2.83$ days, the first-order cracks will be formed in the s_{rml} spacing—that is, there will be a stabilized spacing of the first-order cracks, and the lengths of the local relaxation zones will be reduced to s_{rml} corresponding to a temperature drop from the maximum value by $12.6^\circ\text{C (22.7}^\circ\text{F)}$; therefore; the temperature increase in relation to the temperature of crack initiation is only $1.4^\circ\text{C (2.5}^\circ\text{F)}$. According to Eq. (15),³⁴ for $t_{cr} = 2.83$ days, the following expression was obtained

$$\Delta T_1(t) \approx 12.6^\circ\text{C} \cdot [0.979 / (1.11 \text{ MPa} / 15.8 \text{ GPa})] / [0.883 / (f_{cm}(t) / E_{cm}(t))]$$
(17)

Crack width before stabilized spacing of first-order cracks

According to Eq. (13) and (14)³⁴ and for $L/H = 2.45$, the following expression was obtained

$$w_{k1} = 4H \cdot \overline{\Delta R_{ax}} \left(\frac{0.25L}{L}; \frac{0.75L}{L} \right) \cdot \varepsilon_{free1} \cdot k_{\phi} - \overline{\Delta R_{axAB}} \left(\frac{0.25L}{L}; \frac{0.75L}{L} \right) \cdot (4H - 1.225H) \cdot \varepsilon_{free1} \cdot k_{\phi} \quad (18)$$

in which the average effective degree of relaxation along the wall length with the $L/H = 8$, $\overline{\Delta R_{ax}} (0.25L/L; 0.75L/L) = 0.0239$; $\varepsilon_{free1} = \alpha_T \cdot \Delta T_1(t_{cr}) = 0.00001/^\circ\text{C} \cdot 12.6^\circ\text{C} = 0.126\%$; the average effective degree of relaxation $\overline{\Delta R_{axAB}} (0.25L/L; 0.75L/L)$ along the wall length beyond its physical dimensions—that is, on the difference in lengths between the wall with $L/H = 8$ ($x = 0.25$) and $L/H = 2.45$ ($x = 0.077$). Based on Table 2,³⁵ the degrees of relaxation of ΔR_{ax} ($x = 0.25$) = 0.008 and ΔR_{ax} ($x = 0.077$) = 0.020 were obtained. Hence, the average value $\overline{\Delta R_{axAB}} (0.25L/L; 0.75L/L) = 1/2(\Delta R_{ax}(x = 0.25) + \Delta R_{ax}(x = 0.077)) = 0.014$. By substituting in Eq. (18), the following values ($w_{k1} = 0.059 \text{ mm} - 0.024 \text{ mm} = 0.03 \text{ mm}$ [1.2 mil]) were obtained.

Stabilized spacing of first-order cracks

The average effective degree of relaxation for the segment $-0.5s_{rml}/L$ to $+0.5s_{rml}/L$ was determined based on Table 1.³⁴ After the interpolation for $h_1/H = 0.18$ and $\alpha_D = 1.98/\text{m}$, $\overline{\Delta R_{ax}} (-s_{rml}/2L; s_{rml}/2L) = 0.138$ was obtained.

The limit value of stresses in steel which, if exceeded, will result in the formation of second-order cracks is $\sigma_{sl}^{lim} = k_c \cdot k \cdot f_{cteff}(2.83 \text{ days}) \cdot A_{cl}/A_s = 1.0 \cdot 0.79 \cdot 1.14 \text{ MPa} \cdot 0.6 \text{ m}^2/104.3 \text{ cm}^2 = 51.7 \text{ MPa}$ (7.5 ksi). Thus, based on Eq. (11) or Fig. 10, the limiting crack width was calculated, which can be obtained with the concrete parameters for $t_1 = 2.83$ days close to 0.03 mm (1.2 mil). Therefore, there will be no change in the crack widths in the period of the stabilized spacing of the first-order cracks, but due to the high degree of reinforcement, second-order cracks will be formed.

Changes in crack width during further temperature change

There is a further significant drop in temperature until Day 5.5. This is the period of the formation of the second-order cracks, when the values of the mechanical properties of the concrete increase, and the existing cracks widen.

The change in the difference in average strains in the immediate vicinity of the crack between the steel and concrete during the time interval of 2.83 to 5.5 days cannot be greater than $\Delta(\varepsilon_{sm} - \varepsilon_{cm})_{II}' = 0.179\% - 0.157\% = 0.022\%$ Eq. (20),³⁴ from which according to Eq. (M.1¹) for $t_1 = 2.38$ days, $\alpha(2.38 \text{ days}) = E_s/E_{cm}(2.38 \text{ days}) = 12.41$, $\alpha(5.5 \text{ days}) = E_s/E_{cm}(5.5 \text{ days}) = 11.31$, $k_c = 1.0$, $k = 0.79$, and $\rho = 1.74\%$ were obtained.

In the second stage of loading, until Day 5.5, the average wall temperature was lowered by 29°C (52.2°F). Assuming that the temperature difference between the surface and the inside of the wall is at least 5°C (9°F), $\varepsilon_1 = \alpha_T \cdot (\Delta T + \Delta T_{W-Z}) = 0.00001/^\circ\text{C} \cdot (29^\circ\text{C} + 5^\circ\text{C}) = 0.34 \%$, $\varepsilon_2 = \alpha_T \cdot \Delta T$

$= 0.00001/^\circ\text{C} \cdot 29^\circ\text{C} = 0.29\%$, $k_2 = (\varepsilon_1 + \varepsilon_2)/2\varepsilon_1 = (0.34\% + 0.29\%)/2 \cdot 0.34 \%$ = 0.93 is obtained.

The spacing of the cracks considers ‘poor’ bond conditions according to EN 1992-1-1²: $s_{r,max} = 3.4 \cdot 40 \text{ mm} + 0.425 \cdot 0.8 \cdot 0.94 \cdot 20 \text{ mm}/2.98\% \cdot 0.7 = 0.438 \text{ m}$ (1.44 ft). The increase in the crack width according to Eq. (21)³⁴ is $\Delta w_{k3} = 0.438 \text{ m} \cdot 0.022\% = 0.01 \text{ mm}$ (0.4 mil).

The aforementioned calculations adopted the least favorable data due to s_r^{max} and $\Delta w_{k3}'$. If $\Delta T_{W-Z} = 15^\circ\text{C}$ (27°F) was adopted as on the south side, and ΔT in the initial period of the formation of the second-order cracks—for example, for $t = 2.9$ days, where $\Delta T = 13^\circ\text{C}$ (23.4°F), then $k_2 = (0.28\% + 0.13\%)/2 \cdot 0.28\% = 0.73$ and $s_r^{max} = 0.374 \text{ m}$ (1.23 ft) would be obtained.

Changes in crack width in hardened concrete

The increase in the difference in average strains between the steel and concrete within the time range of 5.5 to 90 days calculated according to Eq. (22)³⁴ is $\Delta(\varepsilon_{sm} - \varepsilon_{cm})_{III}' = 0.261\% - 0.179\% = 0.082\%$. The increase in stresses in reinforcing steel due to external load is $\Delta\sigma_{sII} = N_{sk}/A_s = 170 \text{ kN}/104.3 \text{ cm}^2 = 16.3 \text{ MPa}$ (2.4 ksi), where $N_{sk} = 170 \text{ kN}$ is the maximum tensile force at the h_1 level, for the entire length of the analyzed wall segment from the external load—that is, water pressure during the water-tightness test, defined based on separate FEM calculations using linear analysis.

By applying Eq. (25),³⁴ (26),³⁴ and (24)³⁴ in this order, the following expressions were obtained:

$$\Delta\varepsilon_{sIII} = [16.3 \text{ MPa} - [(0.4 \cdot 1.99 \text{ MPa})/2.98\%] - [(0.4 \cdot 1.99 \text{ MPa})/2.98\%]]/200 \text{ GPa} = 0.082\%,$$

$$\Delta\varepsilon_{cmIII} = [(0.4 \cdot 1.99 \text{ MPa})/22.65 \text{ GPa}] - [(0.4 \cdot 1.99 \text{ MPa})/22.65 \text{ GPa}] = 0\%,$$

$$\Delta(\varepsilon_{sm} - \varepsilon_{cm})_{III}' = 0.082\% - 0.0\% = 0.082\%.$$

In the third stage, the average wall temperature is lowered by 47.6°C (85.7°F). The temperature difference on the surface and inside the wall is 5°C (9°F). In addition, based on the conformity of the shrinkage measurement results and the calculations according to EN 1991-1-1² (refer to Fig. 6), drying shrinkage calculated in accordance with EN 1991-1-1² was adopted in the calculation. It was predetermined that shrinkage at the surface of the member for 90 days of concrete hardening would approximately correspond to the strains that would occur in samples with a cross-section of $0.1 \times 0.1 \text{ m}$. Therefore, for $\text{RH} = 80\%$ and 90 days, drying shrinkage is: $\varepsilon_{cd} = \varepsilon_{cs} - \varepsilon_{ca} = 0.247\% - 0.047\% = 0.20\%$. From the above data, $\varepsilon_1 = \alpha_T \cdot (\Delta T + \Delta T_{W-Z}) = 0.00001/^\circ\text{C} \cdot (47.6^\circ\text{C} + 5^\circ\text{C}) + 0.20\% = 0.726\%$; $\varepsilon_2 = \alpha_T \cdot \Delta T = 0.00001/^\circ\text{C} \cdot 47.6^\circ\text{C} = 0.476\%$; $k_2 = [(\varepsilon_1 + \varepsilon_2)/2\varepsilon_1] \cdot b_1/0.5 \text{ h} = [(0.726\% + 0.476\%)/2 \cdot 0.726\%] \cdot 0.1 \text{ m}/0.5 \cdot 0.6 \text{ m} = 0.276$, in which: $b_1 = 100 \text{ mm}$ (3.9 in.) was read from Table 8.1.⁴²

The spacing of the cracks according to EN 1992-1-1² is $s_{r,max} = 3.4 \cdot 40 \text{ mm} + 0.425 \cdot 0.8 \cdot 0.276 \cdot 20 \text{ mm}/2.98\% \cdot 0.7 = 0.226 \text{ m}$ (0.74 ft). The increase in the crack width from shrinkage according to Eq. (23)³⁴ is $\Delta w_{k3S}'' = 0.226 \text{ m} \cdot 0.082\% = 0.02 \text{ mm}$ (0.8 mil). The increase in the crack width from the external load according to Eq. (27)³⁴: $\Delta w_{k3Z}' = 0.226 \text{ m} \cdot 0.082\% = 0.02 \text{ mm}$ (0.8 mil). The total increase in the crack width after 90 days from the concreting of the wall: $\Delta w_{k3}'' = 0.02 \text{ mm} + 0.02 \text{ mm} = 0.04 \text{ mm}$ (1.6 mil).

COMPARISON WITH EN 1992-3

Due to the lack of the case of a member being restrained along three edges contained in EN 1992-3,¹ the results for the two schemes defined in the standard were presented. The examined properties of the concrete were taken into account in the calculations. For the member restrained at the opposite ends, the widths of the cracks from the imposed load in time $t_{cr} = 4.2, 22.5,$ and 90 days were 0.07, 0.09 and 0.094 mm (2.8, 3.5, 3.7 mil), respectively. For a base-restrained wall, these values were 0.04, 0.07, and 0.13 mm (1.6, 2.8, 5.1 mil), respectively. The crack width from the external load was 0.02 mm (0.8 mil).

According to the model of the base-restrained wall, in the initial period, the widths of the cracks were narrower compared to the member restrained at the opposite ends, but they were comparable to the values obtained according to the proposed model. For $t = 90$ days—that is, having taken the shrinkage of the concrete into account—better conformance with the proposed model was demonstrated by the tie model restrained at opposite edges. According to the authors, in the case of the base-restrained wall, it is contradictory to say that “the formation of a crack in this case only influences the distribution of stresses locally”¹, with the assumption that the spacing of the cracks is according to Eq. (7.11).² According to the authors, this approach to determining the difference in strains according to $R_{ax} \cdot \varepsilon_{free}$ ¹ should be applied to walls that fail to satisfy the condition of the minimum degree of reinforcement. However, in the model of a tie restrained at opposite ends, due to the necessity of also taking imposed strains into account for hardened concrete (for example, shrinkage), the sense of these calculations for thermal loads during concrete hardening (regardless of their value) is undermined because the crack widths obtained are wider with the greater strength of the concrete.

In the proposed model, the obtained spacing between the first-order cracks, compared to those obtained using the approach according to EN 1992-3,¹ is twice as large. In addition, in EN 1992-3,¹ there is some doubt about the lack of any entrance regarding the need to determine the change in the crack widths caused by imposed loads due to the loads occurring later, especially external loads.

DISCUSSION OF RESULTS

The calculated maximum crack width at the individual loading stages is:

- From thermal load in the early period of temperature drop in concrete at the stage of concrete hardening, before the stabilized spacing of the first-order cracks of 0.03 mm (1.2 mil);
- From thermal load in the early period of concrete hardening, before the stabilized spacing of the second-order cracks of 0.03 mm (1.2 mil);
- From thermal load at a later time of temperature drop in concrete at the stage of concrete hardening, at the same time as the period of the formation of the second-order cracks of 0.04 mm (1.6 mil);
- After the occurrence of shrinkage strains in hardened concrete at 0.06 mm (2.4 mil); and

- After the occurrence of external loads in hardened concrete at 0.08 mm (3.1 mil).

The calculations demonstrate that the first cracks will occur on the third day after the concreting of the segment and on the fifth day according to EN 1992-3.¹ This time is consistent with the observations obtained from the object, which demonstrates that the first cracks resulting mainly from concrete temperature drop were formed between the second and third days.

From the calculations performed and the measurements of the crack spacing, one can conclude that just after the first crack was formed, and for a very small value of the increase of the imposed load of 1.4°C (2.5°F), the stabilized spacing of the first-order cracks with the maximum value of 0.79 m (2.6 ft) will be established. This resulting value, from the predetermination of $2H$ in Eq. (17),³⁴ represents the maximum spacing for non-reinforced walls. Given that this spacing usually falls within the range of $1H$ to $2H$, then the observed spacing of the first-order cracks should fall within the range of 0.395 to 0.79 m (1.3 to 2.6 ft). In the calculation model for the period of the stabilized spacing of first-order cracks, according to the calculations, the second-order cracks will start to form, and their maximum spacing decreases to 0.44 m (1.44 ft) (when $t = 2.9$ days and $\Delta T_{w-z} = 15^\circ\text{C}$ (27°F) $s_p^{max} = 0.37$ m is used in the calculations), which further shrinkage decreases to 0.23 m (0.75 ft). The calculated maximum values are greater than the average values observed during the first (Fig. 1) and the second (Fig. A-1) stages by $0.44\text{ m}/0.24\text{ m} = 1.83$ ($0.37\text{ m}/0.24\text{ m} = 1.54$) and $0.226\text{ m}/0.2\text{ m} = 1.13$, respectively. From the computational model, one can conclude that even at the same temperature, the spacing of the first-order cracks may correspond to the spacing of the second-order cracks. Both from the computational model and from the research results, it follows that the spacing of cracks is formed in the initial days of concrete hardening, especially due to the high degree of reinforcement as well as the geometry and how the segment is restrained. These factors brought about a low degree of wall relaxation after cracking, which resulted in the formation of numerous cracks at a very early stage. Therefore, according to the authors, it is difficult to clearly distinguish between the first- and second-order cracks, as could easily be done for the example illustrated in Fig. 9.⁴³ Nevertheless, the study clearly identified longer and wider cracks corresponding to the first-order cracks defined in the model, and those very short and narrow cracks corresponding to the second-order cracks.

The maximal calculated crack width before Day 5.5 was 0.04 mm (1.6 mil), which in the case of the mean values measured from Fig. 5(a) and (b) for the four earliest cracks (Fig. 5(a): 4.5, 4.9, 5.4, 8.8 m [14.8, 16.1, 17.7, 28.9 ft], and Fig. 5(a): 0.9, 5.2, 6.6, 10 m [2.9, 17.1, 21.6, 32.8 ft]) were 0.036 and 0.039 mm (1.42 and 1.54 mil), respectively. However, for the period after the water-tightness test, thermal load in winter, and concrete shrinkage, the calculated crack widths were 0.08 mm (3.1 mil), compared to the values of 0.1 mm (3.9 mil) measured for the vast majority of cases.

According to the calculations, because the crack was formed in the first stage (0.03 mm [1.2 mil]), the crack more

than doubled (0.08 mm [3.1 mil]). Such behavior of the cracks that occur first is consistent with the observations of other objects at a natural scale.^{33,43}

On the basis of the performed calculations, it can also be concluded that apart from the high degree of reinforcement, the most crucial role in crack width restriction is played by the design and actual erecting of the structure in such a way that temperature variations during concrete hardening were the smallest possible; that is, the application of cement of low hydration heat and building the structure in conditions under which it will not suffer from violent temperature changes. The complete algorithm of the model described in Part I³⁴ together with the dependencies used in the present paper is provided in the Appendix in Fig. A-3.

CONCLUSIONS

Based on the results of these research studies on the cracking of semi-massive RC tank walls, the following conclusions can be drawn:

1. The crack widths, measured and calculated over time, increase together with the increase in the imposed load.

2. In the present case, both the computational model and the research results demonstrated a negligible effect of the external load; that is, the pressure of the liquid on the increase in crack widths and the stress of the reinforcing steel.

3. In the case of a high degree of reinforcement, the spacing of the first-order cracks may be comparable to the spacing of the second-order cracks. Then, the smaller but primary increase in the width of the crack that is formed as the first crack occurs with the smaller/more favorable spacing of the second-order cracks. Contrary to popular belief, non-uniform drying shrinkage plays a very advantageous role in the presented example, as it contributes to the reduction of the crack spacing, the increase in their number, and consequently limits the further increase in their widths.

4. To determine the change in crack widths, it is necessary to consider individual types of loads, starting from those occurring at the construction stage of the tank to those from the period of its use.

5. The proposed crack control model distinguishes the type of crack defined herein—that is, the first-order and the second-order cracks and considers the stages of crack formation and the increase in their widths during the subsequent stages of loading.

6. In the case of long semi-massive internal walls, the influence of the imposed load on cracking, compared to the influence of the external load, is essential.

7. Up until now, only DIN EN 1992-1-1/NA³² provides guidelines on taking account of combined impact of imposed deformations and external loads on crack width checking. The present paper, however, is the first to propose stepwise development of crack width covering the specific impacts both in the period of concrete hardening and the operational life of the structure.

8. According to EN 1991-3,¹ the expression $(\epsilon_{sm} - \epsilon_{cm}) = R_{ax} \cdot \epsilon_{free}$ results in the increase in the crack width being largely dependent on the imposed load, without taking into account residual stresses in the wall or its relaxation as a

result of the formation of the crack and the adjacent cracks along the segment length.

9. The results of the studies and the computational model confirmed that cracks that are formed first may more than double in a later period.

AUTHOR BIOS

Mariusz Zych is an Academic at Cracow University of Technology, Krakow, Poland. He received his doctorate of technical sciences at Cracow University of Technology and earned a postdoctoral degree. His research interests include water-tightness and durability of semi-massive reinforced concrete tank walls, early-age cracking, and design and strengthening of reinforced concrete and prestressed tanks for the storage of liquids.

ACI member **Andrzej Seruga** is a Professor of civil engineering. He received his MSc and PhD in civil engineering at Cracow University of Technology. His research interests include post-tensioned and prestressed concrete structures; cracking and water-tightness of special concrete structures (tanks); applications of high-performance concrete to prestressed elements; and strengthening of existing structures, rigid concrete pavements, shotcrete technology, and sulfur concrete.

NOTATION

C_1	= coefficient to include the effect of the creep of the concrete, equal to 0.6
C_2	= 0.8 (value estimated from crack width measurements at the level immediately above restraining base)
c	= cover to longitudinal reinforcement
	= normal stiffness modulus
E_{cm}	= secant modulus of elasticity of concrete
E_s	= modulus of elasticity of reinforcing steel (200 GPa [2.9 Mpsi])
f_b	= mean bond strength
f_{ct}	= tensile strength of concrete
$f_{ct,eff}$	= mean value of tensile strength of concrete effective at time when cracks may be expected to occur: $f_{ct,eff} = f_{ct,cm}(t, T)$
f_{ctm}	= mean value of axial tensile strength of concrete
H	= height of wall
h_1	= height of critical section where cracking occurs first
k	= coefficient that takes into account effect of non-uniform self-equilibrating stresses, which lead to reduction of restraint forces
k_1	= coefficient that takes into account bond properties of bonded reinforcement
k_2	= coefficient that takes into account distribution of strain
	= coefficient that takes into account stress distribution within section immediately prior to second-order cracking
	= coefficient dependent on duration of load
k_ϕ	= 0.65; coefficient that takes into account concrete creep
L	= length of segment wall
N_{sk}	= characteristic value of tensile force from external loads
R	= degree of external restraint
$R_{ax}(\alpha_D)$	= degree of restraint in discrete crack as function of stiffness
R_{ax}^{cr}	= restraint factor for cracked element
R_{ax}^{ncr}	= restraint factor for noncracked element
t_1	= time in which cracks are formed in s_{rm} spacing
α_D	= ratio of stiffness in discrete crack D_{11} to modulus of elasticity of wall, E_{cm}
α_e	= ratio E_s/E_{cm}
α_T	= thermal expansion coefficient of concrete
ΔR_{ax}	= degree of relaxation
	= mean degree of relaxation
$(0.5L/L)$	= mean degree of relaxation for crack spacing 0.5L
(s_{rm}/L)	= mean degree of relaxation for crack spacing s_{rm}
ΔT	= concrete temperature change
ΔT_{cr}	= temperature change resulting in formation of first crack in time equal to t_{cr}
$\Delta \epsilon_{cm1}$	= change in mean strain in concrete between cracks from external loads
$\Delta \epsilon_{sm1}$	= change in mean strain in steel between cracks from external loads
ϵ_{cm}	= mean strain in concrete between cracks
ϵ_{cs}	= shrinkage strain
ϵ_{ctu}	= tensile strain capacity of concrete
ϵ_{free}	= imposed strain
ϵ_{sm}	= mean strain in reinforcement
ϵ_{te}	= thermal strain

ϕ	=	bar diameter
η_1	=	coefficient related to quality of bond condition
ρ	=	degree of reinforcement
$\rho_{p,eff}$	=	effective degree of reinforcement = $A_s/A_{c,eff}$ ($A_{c,eff}$ – as defined in EN 1992-1-1 ²)
σ_s	=	stress in the tension reinforcement after cracking
σ_{sl}	=	additional stress in steel from external load

REFERENCES

- CEN, "Eurocode 2 – Design of Concrete Structures — Part 3: Liquid Retaining and Containment Structures (EN 1992-3)," European Committee for Standardization, Brussels, Belgium, 2006, 23 pp.
- CEN, "Eurocode 2 – Design of Concrete Structures — Part 1-1: General Rules and Rules for Buildings (EN 1992-1-1)," European Committee for Standardization, Brussels, Belgium, 2004, 205 pp.
- CEN, "Eurocode 1990. Basis of Structural Design," European Committee for Standardization, Brussels, Belgium, 2002, 116 pp.
- CEN, "Eurocode 1 – Actions on Structures—Part 1-1: General Actions – Densities, Self-Weight, Imposed Loads for Buildings, (EN 1991-1-1)," European Committee for Standardization, Brussels, Belgium, 2002, 44 pp.
- CEN, "Eurocode 1 – Actions on Structures—Part 1-3: General Actions – Snow Loads, (EN 1991-1-3)," European Committee for Standardization, Brussels, Belgium, 2003, 56 pp.
- CEN, "Eurocode 1 – Actions on Structures—Part 1-5: General Actions – Thermal Actions, (EN 1991-1-5)," European Committee for Standardization, Brussels, Belgium, 2003, 46 pp.
- CEN, "Eurocode 1 – Actions on Structures—Part 4: Silos and Tanks, (EN 1991-4)," European Committee for Standardization, Brussels, Belgium, 2006, 107 pp.
- CEN, "Eurocode 7 – Geotechnical Design—Part 1: General Rules, (EN 1997-1)," European Committee for Standardization, Brussels, Belgium, 2004, 168 pp.
- Beeby, A.W., "A Study of Cracking in Reinforced Concrete Members Subjected to Pure Tension," *Cement and Concrete Association Report 42.468*, 1972, pp. 593-601.
- Scott, R. H., and Gill, P., "Short Term Distribution of Strain and Bond Stress along Tension Reinforcement," *Structural Engineering*, V. 65B, No. 2, 1987, pp. 39-43.
- Beeby, A. W., and Scott, R. H., "Cracking and Deformation of Axially Reinforced Members Subjected to Pure Tension," *Magazine of Concrete Research*, V. 57, No. 10, 2005, pp. 611-621. doi: 10.1680/macr.2005.57.10.611
- Goto, Y., "Cracks Formed in Concrete Around Deformed Tension Bars," *ACI Journal Proceedings*, V. 68, No. 4, Apr. 1972, pp. 244-251.
- Forth, J. P., and Beeby, A. W., "Study of Composite Behavior of Reinforcement and Concrete in Tension," *ACI Structural Journal*, V. 101, No. 2, Mar.-Apr. 2014, pp. 397-406.
- Beeby A.W., and Scott, R. H., "Tension Stiffening of Concrete, Behaviour of Tension Zones in Reinforced Concrete Including Time Dependent Effects," *Supplementary Information TR59*, 2004.
- Beeby, A. W.; Scott, R. H.; and Antonopoulos, A., "Preliminary Results for Long Term Tension Stiffening Effects in Reinforced Concrete Members," *Concrete Floors and Slabs*, R. K. Dhir, M. D. Newlands, and T. A. Harrison, eds., Thomas Telford Publishing, London, UK, 2002, pp. 327-335.
- Clark, L. A., and Cranston, W. B., "The Influence of Bar Spacing on Tension Stiffening in Reinforced Concrete Slabs: *Proceedings of the International Conference on Concrete Slabs*, Dundee, Scotland, 1979, pp. 118-128.
- Floegl, H., and Mang, H. A., "Tension Stiffening Concept Based on Bond Slip," *Journal of the Structural Division*, ASCE, V. 108, No. 12, 1982, pp. 2681-2701.
- Whittle, R., and Jones, T., "Influence of Tension Stiffening on Deflection of Reinforced Concrete Structures," *Technical Report No. 59*, The Concrete Society, Camberley, UK, 2004, 36 pp.
- Vollum, R. L., "Influences of Shrinkage and Construction Loading on Loss of Tension Stiffening in Slabs," *Magazine of Concrete Research*, V. 54, No. 4, 2002, pp. 273-282. doi: 10.1680/macr.2002.54.4.273
- Scott, R. H., and Beeb, A. W., "Long-Term Tension-Stiffening Effects in Concrete," *ACI Structural Journal*, V. 102, No. 1, Jan.-Feb. 2005, pp. 31-39.
- Evans, E. P., and Hughes, B. P., "Shrinkage and Thermal Cracking in a Reinforced Concrete Retaining Wall," *Proceedings of Institution of Civil Engineers*, V. 39, No. 1, 1968, pp. 111-125. doi: 10.1680/icep.1968.8172
- Hughes, P. B., and Miller, M. M., "Thermal Cracking and Movement in Reinforced Concrete Walls," *Proceedings of the Institution of Civil Engineers*, 1970.
- BS, "Design of Concrete Structures for Retaining Aqueous Liquids (8007)," British Standards Institution, London, UK, 1987, 28 pp.
- Al Rhawi, R. S., and Kheder, G. F., "Control of Cracking Due to Volume Change in Base-Restrained Concrete Members," *ACI Structural Journal*, V. 87, No. 4, July-Aug. 1990, pp. 397-405.
- Kheder, G. F., and Fadhil, S., "Strategic Reinforcement for Controlling Volume-Change Cracking in Base-Restrained Concrete Walls," *Materials and Structures*, V. 23, No. 5, 1990, pp. 358-363. doi: 10.1007/BF02472715
- ACI Committee 207, "Effect of Restraint, Volume Change and Reinforcement on Cracking of Mass Concrete (ACI 207)," *ACI Journal Proceedings*, V. 70, No. 7, July 1973, pp. 445-470.
- Harrison, T. A., "Early-Age Thermal Crack Control in Concrete," *CIRIA Report 91*, 1981, 48 pp.
- BS 5337, "Code of Practice for the Structural Use of Concrete for Retaining Aqueous Liquids," British Standards Institution, London, UK, 1976.
- Kheder, G. F.; Al-Rawi, R. S.; and Al-Dhahi, J. K., "A Study of the Behavior of Volume Change Cracking in Base Restrained Concrete Walls," *Materials and Structures*, V. 27, No. 7, 1994, pp. 383-392. doi: 10.1007/BF02473441
- Klemczak, B., and Knoppik-Wróbel, A., "Degree of Restraint Concept in Analysis of Early-Age Stresses in Concrete Walls," *Engineering Structures*, V. 102, No. 11, 2015, pp. 369-386.
- Zych, M., "Analysis of RC Tank's Walls during Early Hardening Period of Concrete, in Aspect of Water-Tightness," doctoral thesis, Division of Structural Engineering, Cracow University of Technology, Krakow, Poland, 2011, 246 pp.
- Eurocode 2, "Bemessung und Konstruktion von Stahlbeton- und Spannbetontragwerken – Teil 1-1: Allgemeine Bemessungsregeln und Regeln für den Hochbau (DIN EN 1992-1-1:NA2011-01)," Nationaler Anhang, Berlin, Germany, 2011.
- Seruga, A., and Zych, M., "Research on Thermal Cracking of a Rectangular RC Tank Wall under Construction. I: Case Study," *Journal of Performance of Constructed Facilities*, V. 30, No. 1, 2016, pp. 1-10. doi: 10.1061/(ASCE)CF.1943-5509.0000704
- Zych, M., "A New Model of Crack Control in Reinforced Concrete Tank Walls—Part I: Analytical Investigation," *ACI Structural Journal*, V. 116, No. 3, May 2019, pp. 1-10.
- Zych, M., "Degree of External Restraint of Wall Segments in Semi-Massive Reinforced Concrete Tanks: Part I Rectangular Segments," *Structural Concrete: Journal of fib*, V. 19, No. 3, 2018, pp. 820-828. doi: 10.1002/suco.201700036
- Klemczak, B., and Knoppik-Wróbel, A., "Analysis of Early-Age Thermal-Shrinkage Stresses in Reinforced Concrete Walls," *ACI Structural Journal*, V. 111, No. 2, Mar.-Apr. 2014, pp. 313-322.
- Zych, M., "Thermal Cracking of the Cylindrical Tank under Construction. II: Early Age Cracking," *Journal of Performance of Constructed Facilities*, V. 29, No. 4, 2015, pp. 1-10. doi: 10.1061/(ASCE)CF.1943-5509.0000577
- Bamforth, P. B., "Early-Age Thermal Crack Control in Concrete," *CIRIA Report C660*, London, UK, 2007.
- Pettersson, D., and Thelandersson, S., "Crack Development in Concrete Structures Due to Imposed Strains. Part I: Modelling," *Materials and Structures*, V. 34, No. 1, 2001, pp. 7-13. doi: 10.1007/BF02482194
- Volkersen, O., "Distribution of Forces Inrivet Joints under Tensile Loading," *Luftfahrtforschung*, V. 35, 1938, pp. 41-47.
- Zych, M., "Degree of External Restraint of Wall Segments in Semi-Massive Reinforced Concrete Tanks: Part II: Rectangular and Cylindrical Segments," *Structural Concrete: Journal of fib*, V. 19, No. 3, 2018, pp. 829-838. doi: 10.1002/suco.201700037
- Flaga, K., "Shrinkage Stresses and Surface Reinforcement in Concrete Structures" Monograph 391, Cracow University of Technology, Krakow, Poland, 2011.
- Seruga, A., and Zych, M., "Thermal Cracking of the Cylindrical Tank under Construction. I: Case Study," *Journal of Performance of Constructed Facilities*, V. 29, No. 4, 2015, pp. 1-9. doi: 10.1061/(ASCE)CF.1943-5509.0000581

ACI Research and Academic Opportunities

This article details some of the opportunities for researchers and professionals upon becoming a part of the ACI community. This article will outline the possibilities available to members, such as attending The ACI Concrete Convention and Exposition, viewing past technical presentations, access to a vast abstract library, and ACI's Call for Papers. Up-to-date information concerning these and additional opportunities can be found at ACI's website, www.concrete.org.

THE ACI CONCRETE CONVENTION AND EXPOSITION

ACI Conventions give attendees the opportunity to participate in the development of industry codes and standards, learn about the latest in concrete technology, network with leading concrete professionals, and fulfill potential continuing education requirements.

ACI technical and educational sessions, which are held during ACI Conventions, provide attendees with the latest research, case studies, best practices, and opportunities to earn Professional Development Hours and Continuing Education Units. ACI committees, whose meetings take place during the ACI Convention, develop the standards, reports, and other documents needed to keep those in the industry up to date with the latest technology. Committee meetings are open to all registered convention attendees.

The ACI Convention takes place twice a year—once in the fall and once in the spring. ACI reserves rooms at local hotels and offers a discounted rate to members. Networking and other nontechnical events are coordinated through ACI and take place at each convention.

TECHNICAL PRESENTATIONS AND DOCUMENTS

Access to a vast abstract library, online educational presentations, webinars, and ACI education documents are often free for members or offered at a discounted rate. New presentations and documents are always being added.

CALL FOR PAPERS

ACI is accepting the submission of papers for conventions, committees, chapters, and subsidiaries. Detailed

ACI Convention Schedule

City	Location	Dates
Cincinnati, OH, USA	Duke Energy Convention Center & Hyatt Regency Cincinnati	October 20-24, 2019
Rosemont, IL, USA	Hyatt Regency O'Hare	March 29-April 2, 2020
Raleigh, NC, USA	Raleigh Convention Center & Raleigh Marriott	October 25-29, 2020
Baltimore, MD, USA	Hilton & Marriott Baltimore	March 28-April 1, 2021
Atlanta, GA, USA	Hilton Atlanta Downtown	October 17-21, 2021
Orlando, FL, USA	Caribe Royale Orlando	March 27-31, 2022
Dallas, TX, USA	Hyatt Regency Dallas	October 23-27, 2022

descriptions of submission requirements and policies can be found at www.concrete.org. ACI's website also contains a detailed list of the date(s), sponsor(s), and location(s) of events calling for papers.

Guidelines for submitting technical papers for review to either the *ACI Structural Journal* or the *ACI Materials Journal* can be found at ACI's website.

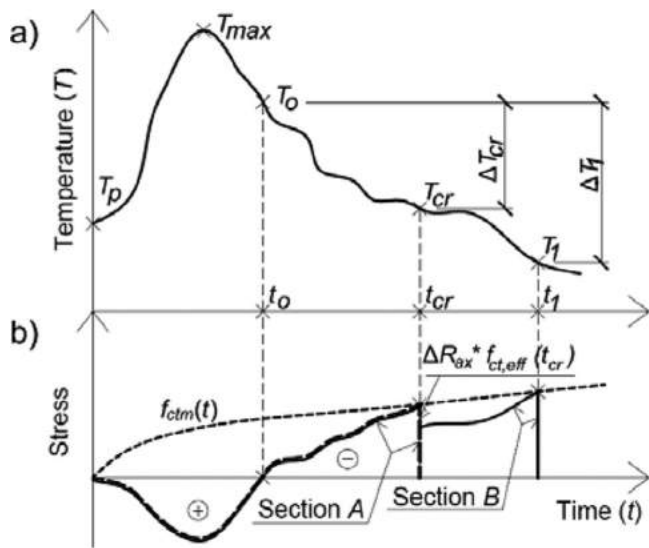


Fig. 1—(a) Exemplary changes in average wall temperature during concrete hardening; and (b) development of horizontal stresses in critical sections resulting from temperature changes.

on the crack width calculation was introduced with certain restrictions in DIN EN 1992-1-1/NA.²⁵ This approach is fully based on equations defined in EN 1992-1-1.⁹

RESEARCH SIGNIFICANCE

This research paper is important for the crack control and water-tightness of semi-massive reinforced concrete tank walls, in which cracking may occur at the construction stage and develop later as a result of imposed deformation or external loads. The stepwise development of the crack width is not defined in EN 1992-3⁴ or in the world literature and is a new concept of the proposed model. The results of this study can serve as a basis for future code changes for crack control derived from hydration temperatures, elevated temperatures, shrinkage, and external load effects on crack propagation.

MODEL ASSUMPTIONS

Crack control must be performed, especially in critical sections subjected to the greatest tensile stresses during the cooling period. The sections are located at the height h_1 from the connection to the foundation (Sections 1²⁶ and 2²⁶) corresponding to the height at which the wall temperature profile changes from linear to uniform.

Figure 1(a) illustrates an average temperature change in the wall section and the corresponding change in the concrete stress. A simplification is often used consisting of completely leaving out the compressive stress occurring during the temperature increase due to the low level of this stress. However, the level of tensile stress is also relatively low. Therefore, in the author's opinion, it is equally reasonable to adopt the coefficient k_σ representing the ratio of compressive stress in the period of temperature increase to tensile stress in the period of its decrease determined for the first days of concrete hardening. Zych²⁷ presented that, for real conditions of implementing construction, the

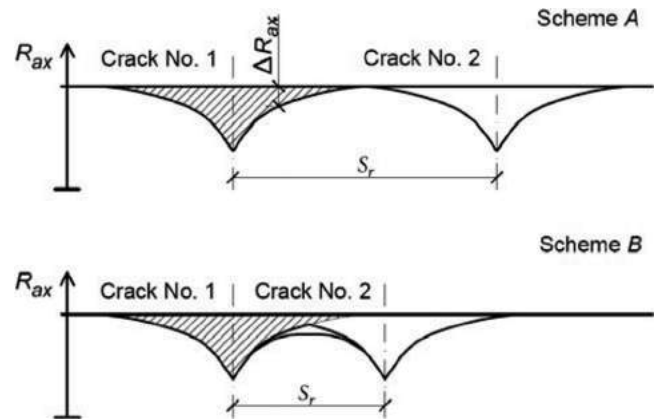


Fig. 2—Reduced degree of restraint depending on crack spacing.

proportions of compressive and tensile stresses just before the first cracks occur are strongly dependent on solar radiation, and it makes the levels of both stresses on the outer and inner surfaces of the cylindrical wall segment vary by nearly 100%. Due to the high variability in the coefficient k_σ depending on, for example, the cement type, external conditions, water curing method, degree of external restraint, and cracking time, according to the author, it is recommended to adopt a safe value of $k_\sigma = 0.2$ corresponding to a 20% reduction in the tensile stress due to earlier compressive stress.

Figure 1(b) illustrates the development of stress in the critical cross section “A”, where the first cracks occur in a given segment. At the moment of their occurrence, the restrained part of the strain in the local relaxation zone decreases. Hence, the stress in the “B” cross section located at the same level h_1 and in the relaxation zone of the first crack is suddenly reduced. A crack at this cross section may occur with a further significant temperature drop, during which the mechanical properties of concrete also increase. Considering only the imposed deformation, it can be assumed that the formation of subsequent cracks will cause a decrease in the degree of restraint and a less effective increase in the widths of the existing cracks. This fact is taken into account by introducing a reduction in the restrained part of the increment of imposed strain by the quantity according to the following formula (refer to Fig. 1(b))

$$\Delta \varepsilon = \Delta R_{ax} \cdot \frac{f_{ct,eff}(t_{cr})}{E_{cm}(t_{cr})} \quad (1)$$

The range of the relaxation zones²⁴ comprises the area where the occurrence of the next cracks is most likely. Figure 2 demonstrates two basic cases of a possible location for the first cracks with respect to each other. In the first one (Fig. 2(a)), the crack spacing is greater than or equal to the length of the concrete relaxation zone. In this case, the width of the cracks is affected by the entire relaxation zone. In the second case (Fig. 2(b)), where the crack spacing is smaller, the concrete relaxation zones overlap, which means that smaller crack widths can be expected. The model considers the entire concrete relaxation zone to determine the width

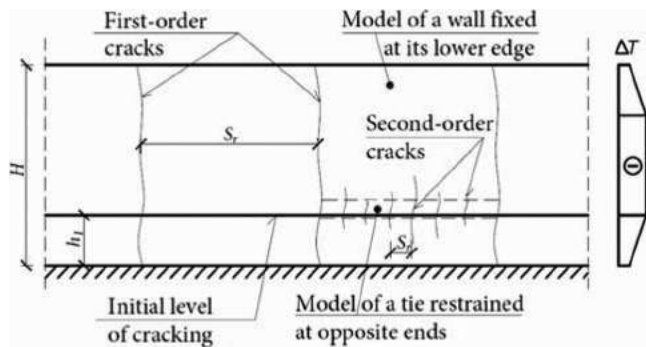


Fig. 3—Computational model assumptions concerning initial level of occurrence of first-order cracks.

of the crack that occurs first. In the case of crack No. 2, the relaxation zone shaping the crack width is smaller.

Zych²⁶ presented the influence of changing the temperature profile on the degree of restraint at different values of h_1/H . The material tests²⁸ were carried out on the concrete used for the implementation of semi-massive reinforced concrete tank walls. A modulus of elasticity was obtained after 1 day from the time after which segment cooling could commence equal to approximately 1/3 of the 28-day value. Hence, when determining the degree of restraint, a constant ratio was assumed by author of 1/3 the concrete elasticity modulus in the wall segment to its elasticity modulus in the previously executed segments. Generally, this ratio depends on the technological break between concreting of the wall and the foundation.

In this model, the degree of reinforcement in the construction joints between wall segments is taken into consideration of the degree of external restraint (Section 3²⁶).

From the existing models and observations performed on objects at the natural scale,^{29,30} it can be concluded that the crack spacing should fall within the range of cases defined in EN 1992-3⁴ and by Iványi⁶ as well as Rostásy and Henning.⁷ In general, the crack spacing for each of these models is not, however, a set of stabilized cracks and, in most cases, is rarely final. It is the spacing of cracks at a given stage of a load or its type. According to the author, the spacing of cracks defined in EN 1992-1-1⁹ (Eq. 7.11⁹) can occur only in walls with a very high degree of horizontal reinforcement because it will not depend on the restraint scheme but rather almost exclusively on the degree of reinforcement restraining the concrete strain. In such a spacing, second-order cracks (Fig. 3) may occur between first-order cracks and only in some cases affect the water-tightness of the tank walls.

In view of the aforementioned statements, the next model assumption is the adoption of three basic stages for determining the crack widths (refer to Fig. 4):

- **Stage I** concerns the occurrence of the first cracks w_{k1} from imposed strains ϵ_{free1} in the initial period when the primary relaxation zones do not overlap.
- **Stage II** concerns the stabilized spacing of first-order cracks and the initial period of the imposed strains ϵ_{free2} during which the cracks from Stage I become wider ($w_{k2} = w_{k1} + \Delta w_{k2}$).

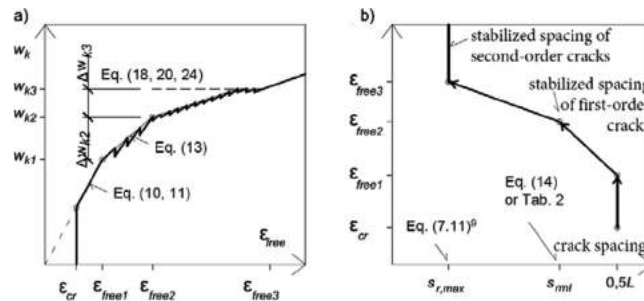


Fig. 4—(a) Changes in crack width; and (b) changes in their spacing as a function of imposed loads.

- **Stage III** concerns large imposed strains or mostly service loads (ϵ_{free3}), causing second-order cracks and at the same time an increase in the widths of the cracks from the previous stages ($w_{k3} = w_{k2} + \Delta w_{k3}$).

In-place research studies

Based on the results of a previous study,³¹ it can be concluded that cracks were formed at $h_1 = 1.1$ m on the outer surface of this segment with a much higher degree of reinforcement; however, they were definitely narrower and shorter, and their increment over time was much more limited. Therefore, Fig. 4 presents the general assumptions in the proposed model regarding the changes in the crack width and spacing as a function of a progressively imposed load. It also demonstrates that an increment of the imposed strain ϵ_{free} will result in a continuous increase in the crack width (Fig. 4(a)) and a continuous decrease in the crack spacing (Fig. 4(b)) until they stabilize, which in practice is extremely rare for reinforced concrete tank walls. Assuming that f_{cm} is constant, with an increase in ϵ_{free} , a steady increase in the number of cracks will occur. In contrast, considering $f_{cm}(t)$, a larger increase in first-order crack widths w_{k1} will be observed with a smaller number of newly formed cracks. Having reached f_{cm} ($t = 28$ days) in the first stage with an increase in ϵ_{free} , there will be a further increase in the crack width w_{k1} with a constant spacing s_{rml} , and in the subsequent stage, a further reduction in the crack spacing will be observed until it has stabilized. Therefore, in the case of the cracks formed in the early stages of concrete hardening, their widths w_{k1} increase by Δw_{k2} as a result of the loads occurring at higher concrete mechanical properties. In the studies of Ouzaa and Benmansour,³² it was confirmed that the first cracks were the widest and developed in later stages when other, narrower cracks were formed.

The presented in-place research studies and observations of tank cracking form the grounds for drawing conclusions about the distribution of cracks and their type. Seruga and Zych³⁰ presented a typical type of cylindrical tank wall segment inner surface cracking. In this case, four first-order cracks of basic length and width are clearly visible, and the remaining second-order cracks are definitely narrower and shorter. Out of the four examined structures of this type, a similar crack layout could be observed on almost all internal surfaces of these cylindrical segments.³³

Observations also confirm the necessity of including an appropriate height h_1 —that is, the height of the initial level

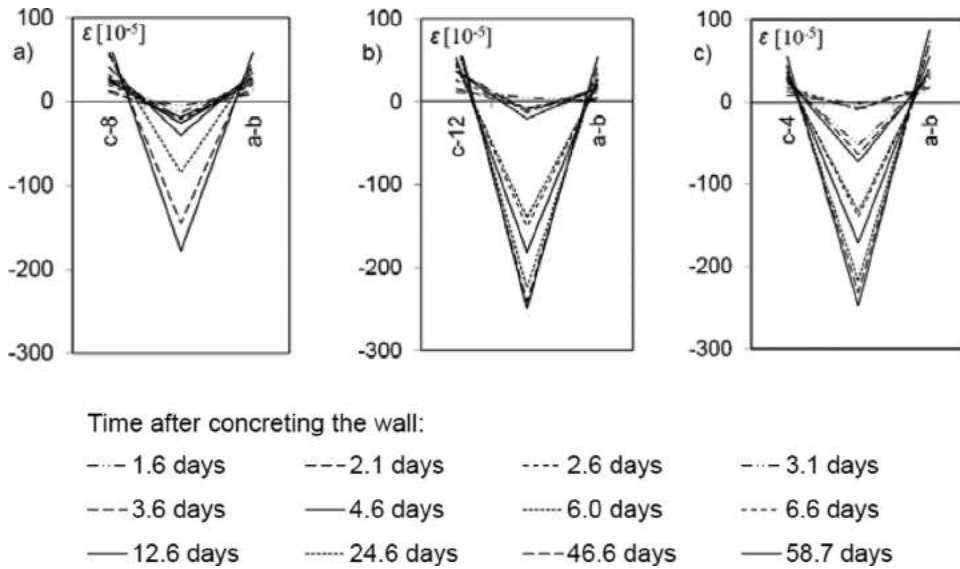


Fig. 5—Changes in strains in cracked sections, denoted as: (a) S1³⁰; (b) S5; and (c) S6.

of crack occurrence—in the analytical models. In this case,³⁰ it was the level of 1.1 m at which the first cracks occurred and developed significantly upward and downward later on. At the same level, second-order cracks occurred at a later stage as well.

To carry out quantitative and qualitative observations of the increase in the crack widths, Fig. 5 illustrates exemplary detailed results of the measurement of strains that are presented in a more general form by Seruga and Zych.³⁰ The measurement of strain resulting from imposed deformation was made at the level of 1.1 m in sections through the cracks marked as S1, S5, and S6.³⁰ This strain forms the basis for determining changes in the crack width (S1 to S6) as a function of time (Fig. 6). Thus, the largest increase in the crack width is accompanied by the largest change in the imposed load in the absence or a limited number of second-order cracks. Later, with a smaller imposed load and a larger number of second-order cracks, the increment of the first-order crack width is much smaller. The example of cracks³⁰ due to the eccentric shell tension and related redistribution of strain after cracking (Section 3²⁴) together with a low degree of inner surface reinforcement and a higher degree of outer surface reinforcement is a more complex issue than the case of straight, symmetrically reinforced walls. Nevertheless, it can be concluded that the increment of first-order crack widths from imposed loads is not limited to the early-age thermal loads and that the formation of further cracks does not limit the increase in the widths of earlier cracks. More importantly, it can be concluded that the increase in crack widths from imposed loads may also occur with the mechanical properties of concrete that are higher than the 28-day ones resulting from the extended curing time of concrete made with the additive of blast-furnace slag (refer to Fig. 6).

Moreover, subject to the strain measurement based on S3 to S6,³⁰ the increments of the crack widths were determined (Fig. 7). The measurements prove that significant increases in the crack width and height occur for the entire crack height over the entire period of the imposed load—that is, up to the 60th day after concreting the wall.

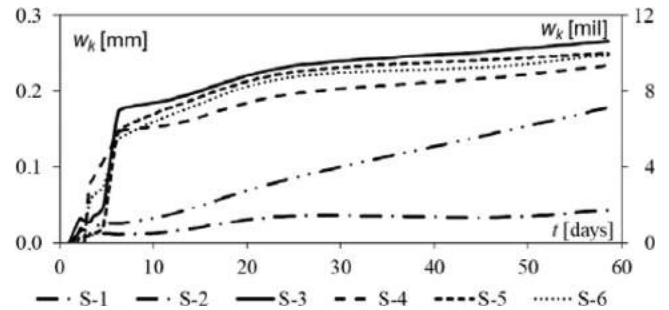


Fig. 6—Changes in crack width over time, denoted as S1³⁰ through S6³⁰, determined from measured strains as illustrated in Fig. 5. (Note: 1 mm = 0.0394 in.)

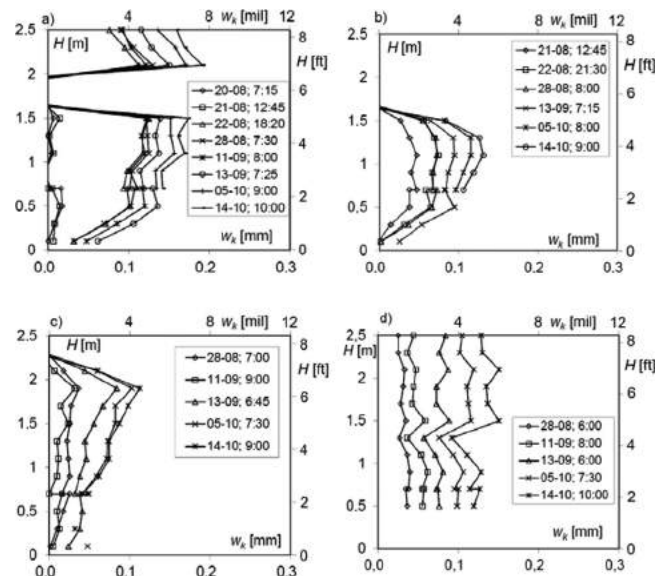


Fig. 7—Increase in crack width over time as determined from measured strains on grids denoted as S3³⁰ to S6³⁰. (Note: 1 m = 3.28 ft; 1 mm = 0.0394 in.)

ANALYTICAL INVESTIGATION

The change in the degree of restraint along the segment length depends mainly on the stiffness of external restraints. This depends not only on the stiffness of neighboring segments but also, to a large extent, on the degree of reinforcement in construction joints. Immediately after cracking, the degree of restraint R_{ax} is reduced depending on the degree of wall reinforcement at the point of cracking. According to the author, the redistribution of strain observed from changing the restraint degree after cracking forms the basis for determining a part of the strain known as the free strain, which accumulates in cracks and forms the basis for calculating their width. Figure 8 illustrates an example of the change in the restraint degree resulting from a crack. A decrease in the restraint degree, hereinafter referred to as the degree of relaxation ΔR_{ax} , is largest in the immediate vicinity of the crack, and it goes to zero as it moves away from its section. With a further increment in the imposed load, another crack may form outside the local relaxation zone or within it, where the ratio of the degree of restraint R_{ax}^{cr} to the tensile strength of concrete is the greatest. The presented case is characteristic of reinforced concrete tank wall segments. In the tie model, which is restrained at its ends only, the same value of relaxation will be present along the entire length of the member.³⁴

The degree of relaxation ΔR_{ax} falls within the range from 0 to R_{ax} (Fig. 8 and 9) and can be defined as the value corresponding to the reduction in the degree of restraint (Eq. (2)). A value of 0 means no relaxation and no cracks. The value of $\Delta R_{ax} = R_{ax}$ means total relaxation that can occur only in the immediate vicinity of the crack in a non-reinforced member. Figure 9 illustrates the changes in the relaxation degree along the length of the segment calculated in the finite element method (FEM) model using different degrees of reinforcement for cases analogous to those in Section 2²⁴ according to Eq. (2). In reinforced concrete walls, the range of these changes depends on the relative height h_1/H of the initial level of crack occurrence and on the stiffness of the cracked section D_{11} .²⁴ Restraint factors R_{ax}^{uncr} and R_{ax}^{cr} used in the proposed model are based on the approach presented by Zych.^{24,26}

$$\Delta R_{ax}(x/L) = R_{ax}^{uncr}(x/L) - R_{ax}^{cr}(x/L) \quad (2)$$

The relative value of the unit width of the crack w_k/L that is formed first can be written as follows

$$W_{\Delta R_{ax}} \left(\alpha_D; \frac{h_1}{H} \right) = \frac{\hat{w}_k}{0.5L} = \int_{\zeta_1 = -s_r/2L}^{\zeta_2 = s_r/2L} \Delta R_{ax}(x/L) d\zeta \quad (3)$$

where $\zeta = x/L$; $s_r = 0.5L$; $\alpha_D = D_{11}/E_{cm}$; and \hat{w}_k is the unit crack width.

Substituting Eq. (4)²⁶ into Eq. (1),²⁶ the distribution of spring stiffness takes the form

$$k_r(\sigma_s) = \frac{\sqrt{\frac{k_b(\sigma_s) \cdot E_s}{\phi}} \cdot \rho_{p,eff}}{\tanh(\lambda a)} \quad (4)$$

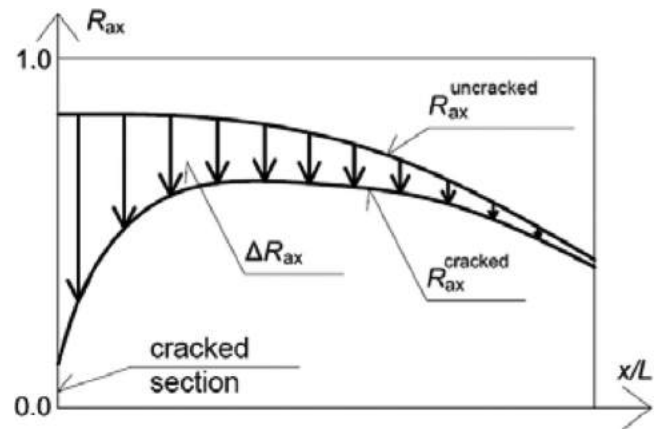


Fig. 8—Degree of relaxation ΔR_{ax} after cracking.

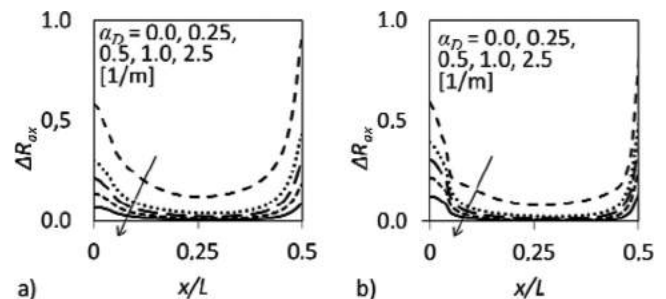


Fig. 9—Effective degree of relaxation ΔR_{ax} of segment restrained at three edges at height h_1 after cracking in joint construction and in segment axis for (assumptions as in 2,²⁴ load of decreased temperature as in Fig. 3 in vertical and horizontal directions): (a) $h_1 = 0.2H$; (b) $h_1 = 0.1H$ (structural joint $x/L = 0$, crack in segment axis $x/L = 0.5$). (Note: $1/m = 0.305/\text{ft}$.)

in which λ is expressed as

$$\lambda = \sqrt{\frac{k_b \cdot \pi \cdot \phi}{E_s \cdot A_\phi}} \quad (5)$$

Stiffness in a discrete crack D_{11} as a function of: concrete class, its maturity, strain time, as well as the degree of reinforcement, and reinforcement bar diameter can be defined on the basis of the assumptions included in EN 1992-1-1.⁹ Thus, distributed bond-slip stiffness along a given reinforcement bar as a function of stresses in reinforcement bar can be defined, as the maximum bond stress value (Eq. (9))²⁶ divided by crack width (Eq. (6))²⁶

$$k_b(\sigma_s) = \frac{f_{bk}(\sigma_s)}{w_k(\sigma_s)} \quad (6)$$

In Eq. (3), it was predetermined that the relative value of the unit crack width is considered—that is, the value independent of the strain describing the width of the crack that occurs first in the middle of the wall segment length; hence, $s_r = 0.5L$. Moreover, the basis for determining the crack width is the degree of relaxation occurring within the limits of ζ_1 , and ζ_2 dependent on s_r , beyond which the degree of relaxation is attributed to neighboring cracks. Therefore, the

Table 1—Values of mean wall relaxation $\overline{\Delta R_{ax}} (0.5L/L) / \overline{\Delta R_{ax}} (s_{rml}/L)$ for unit value of ϵ_{free} as well as for crack spacing $0.5L$ and s_{rml} (according to Eq. (9))

$\alpha_D \cdot 1 \text{ m}$	Relative height of initial level of cracking h_1/H			
	0.05	0.1	0.2	0.4
0	0.1036/0.3105	0.1744/0.3710	0.2793/0.4852	0.3855/0.5685
0.25	0.0587/0.2835	0.0836/0.3167	0.1115/0.3155	0.1295/0.3068
0.5	0.0441/0.2610	0.0584/0.2793	0.0725/0.2500	0.0795/0.2029
1.0	0.0305/0.2260	0.0373/0.2203	0.0431/0.1750	0.0451/0.1222
1.5	0.0236/0.1976	0.0277/0.1767	0.0308/0.1290	0.0315/0.0898
2.0	0.0193/0.1735	0.0220/0.1472	0.0239/0.1031	0.0242/0.0703
2.5	0.0164/0.1542	0.0183/0.1261	0.0196/0.0860	0.0196/0.0578
∞	0.00	0.00	0.00	0.00

Notes: h_1 is height corresponding to change in temperature profile from linear to constant; $1 \text{ m} = 3.28 \text{ ft}$.

width of the first-order cracks just before their spacing stabilizes is

$$w_{\Delta R_{ax}}(\alpha_D; h_1/H) = W_{\Delta R_{ax}}(\alpha_D; h_1/H) \cdot L \cdot \epsilon_{free1} \quad (7)$$

Alternatively, it can be written as

$$w_{\Delta R_{ax}}(\alpha_D; h_1/H) = 0.5L \cdot \overline{\Delta R_{ax}}(x/L) \cdot \epsilon_{free1} \quad (8)$$

where

$$\overline{\Delta R_{ax}}(s_r/L) = \frac{1}{\zeta_2 - \zeta_1} \int_{\zeta_1 = -s_r/2L}^{\zeta_2 = s_r/2L} \Delta R_{ax}(\zeta) d\zeta \quad (9)$$

in which, for the first crack formed, $s_r = 0.5L$; and $s_r = s_{rml}$ with the stabilized spacing of first-order cracks.

Then, the value representing the difference between the average strain of steel and concrete for the case of one crack in the middle of the wall segment length and the cracks in the segment construction joint can be determined from the following dependence

$$(\epsilon_{sm} - \epsilon_{cm}) = \epsilon_{free1} \cdot \frac{1}{0.25L/L} \cdot \int_{\zeta_1 = -\frac{0.25L}{L}}^{\zeta_2 = \frac{0.5L}{L}} \Delta R_{ax}(D_{11}/E_{cm}; \zeta) \cdot d\zeta \quad (10)$$

where $R_{ax}(D_{11}/E_{cm}; \zeta)$ is the distribution of the effective degree of relaxation along the segment length ($\zeta = x/L$) for the case corresponding to the fixed stiffness in the structural joint.

Then, the mean value of the effective degree of restraint change $\overline{\Delta R_{ax}}$ at the section of the relaxation zone from $0.25L/L$ to $0.75L/L$ while assuming that $L/H = 8$ and $s_r = 0.5L$ can be defined as

$$\overline{\Delta R_{ax}}\left(\frac{0.25L}{L}; \frac{0.75L}{L}\right) = 4 \cdot \int_{\zeta_1 = 0.25}^{\zeta_2 = 0.75} \Delta R_{ax}(D_{11}/E_{cm}; \zeta) \cdot d\zeta \quad (11)$$

Width of first crack

The width of the first crack can be written according to the following well-known relationship (EN 1992-1-1⁹)

$$w_k = s_r \cdot (\epsilon_{sm} - \epsilon_{cm}) \quad (12)$$

Assuming that its width depends on the entire relaxation zone from $0.25L/L$ to $0.75L/L$ —that is, $s_r = 0.5L$, it can be written

$$w_{k1} = 4H \cdot \overline{\Delta R_{ax}}(0.25L/L; 0.75L/L) \cdot \epsilon_{free1} \cdot k_\phi \quad (13)$$

If the quantity $\overline{\Delta R_{ax}}(0.25L/L; 0.75L/L)$ is used for the walls with the ratio of $L/H = 8$ (Table 1), an adjustment is required for the walls with the ratio of $L/H < 8$. Therefore, the value of the above expression should be reduced by

$$\overline{\Delta R_{ax}}\left(\frac{L/H|_{real} \cdot H}{L}; \frac{8H}{L}\right) \cdot \left[4H - \frac{L/H|_{real} \cdot H}{2}\right] \cdot \epsilon_{free1} \cdot k_\phi \quad (14)$$

in which $k_\phi = 0.65$ was adopted after CIRIA,³⁵ which takes into account the favorable effect of concrete creep reducing the values of the stresses, strains and consequently the crack width $\epsilon_{free1} = \alpha_T \cdot \Delta T_1(t_1)$, and $\Delta T_1(t_1)$ is the temperature change that generates a tensile stress until the next crack in the local stress zone is formed. It can be determined using a simplified expression

$$\Delta T_1(t_1) \approx \Delta T_{cr}(t_{cr}) \cdot \frac{R_{ax}^{ucr}(0.5L)/\epsilon_{ctu}(t_{cr})}{R_{ax}^{cr}(s_{rml}/2)/\epsilon_{ctu}(t_1)} \quad (15)$$

Increase in width during stabilized spacing of first-order cracks

After the occurrence of additional imposed loads, new cracks form that will shorten the local relaxation zone initially assigned to the first crack. This case will occur when $\Delta T > \Delta T_1$, and hence, for $s_{rml} < 0.5L$, it is obtained as follows

$$w_{k2} = w_{k1} + \Delta w_{k2} = w_{k1} + s_{rml} \cdot \overline{\Delta R_{ax}} \left(\frac{-s_{rml}}{2L}; \frac{s_{rml}}{2L} \right) \cdot \left(\varepsilon_{free2} - \frac{\Delta R_{ax} \cdot f_{ct,eff}}{E_{cm}(t_{cr2})} \right) \cdot k_{\phi} \quad (16)$$

where ΔR_{ax} is relaxation that occurs at the cross section of the first crack after the second crack is formed.

The use of a two-stage crack width determination—that is, w_{k1} and its increment Δw_{k2} —is necessary for two reasons. The first one results from the occurrence of an imposed load that is so low that only one crack can form in this specific area that will accumulate the entire free strain. In the second case, the imposed load builds up gradually and, in the relaxation zone of the first crack, the occurrence of the next crack is significantly shifted in time. Then, due to the lower-bond strength from concrete to steel, the first crack accumulates the greatest free strain and relaxes the wall the most. The subsequent cracks shall not contribute to the reduction in the width of the original crack but rather to a smaller increase in its width, which is taken into consideration by the shorter relaxation zone and the value of $\Delta\varepsilon$, as in Eq. (1).

Table 1 demonstrates the values of $\overline{\Delta R_{ax}}$ ($0.5L/L$) for individual crack stiffnesses $D_{11} = \alpha_D/E_{cm}$. Comparing them with the standard values of the R_{ax} coefficient (Fig. L.1⁴ and Table L.1,⁴ which take into account the favorable creep effect), it can be concluded that the proposed values representing the difference in strain between steel and concrete for the unit values of ε_{free} and using the coefficient $\overline{\Delta R_{ax}}$ are much smaller (compare with Eq. (M.3)⁴). The difference in strain is significantly reduced with the increased degree of reinforcement at the crack point, and even in the case of $\alpha_D = 0$, the obtained values are not close to the standard values of the R_{ax} coefficient = 0.5. Moreover, this value represents effective restraint R_{ax} , which takes into account sustained loading and creep. This comparison of two completely different coefficients is valid only for the manner of determining the value of $(\varepsilon_{sm} - \varepsilon_{cm})$ defined in EN 1992-3.⁴

As the value of h_1/H increases, higher values of $\overline{\Delta R_{ax}}$ are observed, indicating greater relaxation and wider cracks. The influence of the h_1/H value on $\overline{\Delta R_{ax}}$ disappears with an increasing degree of reinforcement. Thus, the expression $(\varepsilon_{sm} - \varepsilon_{cm}) = R_{ax} \cdot \varepsilon_{free}$ contained in EN 1992-3,⁴ in which $L/H = 8$ and $R_{ax} = 0.5$, should be considered conservative.

Spacing of first-order cracks

The size and range of the relaxation zone determines not only the widths but also the spacing of the cracks. According to the assumptions contained in the models^{6,7} that the spacing of the dilatation cracks is $(1/2)H$ for the case of a non-reinforced wall and $h_1 = 0.4H$, this paper adopted the spacing of first-order cracks equal to $2H$ as the limit value. The maximum considered value of h_1/H results from the fact that the higher the initial level of the crack occurrence is, the greater and more extensive the wall relaxation directly affecting the large crack spacing. The mean value of wall relaxation $\overline{\Delta R_{ax}}$ ($0.5 L/L$) for this case is 0.3855 (Table 1). Assuming that, after a thermal crack, the sum of the free part of imposed strain over the entire length of the segment is

Table 2—Relative spacing of first-order cracks s_{rml}/H (resulting from external restraints and crack stiffness) as function of mean wall relaxation $\overline{\Delta R_{ax}}$ according to Eq. (17)

$\alpha_D \cdot 1 \text{ m}$	Relative height of initial level of cracking h_1/H			
	0.05	0.1	0.2	0.4
0	0.537	0.905	1.449	2.000
0.25	0.305	0.433	0.579	0.672
0.5	0.229	0.303	0.376	0.413
1.0	0.158	0.194	0.224	0.234
1.5	0.122	0.143	0.160	0.163
2.0	0.100	0.114	0.124	0.125
2.5	0.085	0.095	0.102	0.102
∞	—	—	—	—

Notes: h_1 is height corresponding to change in temperature profile from linear to constant; 1 m = 3.28 ft.

equal for each individual case, the spacing between the cracks was determined according to the following relationship

$$s_{rml} = 2H \frac{\int_{\zeta_1=0.25}^{\zeta_2=0.5} \overline{\Delta R_{ax}}(\alpha_D; h_1; \zeta) \cdot d\zeta}{\int_{\zeta_1=0.25}^{\zeta_2=0.5} \overline{\Delta R_{ax}}(\alpha_D = 0; h_1 = 0.4H; \zeta) \cdot d\zeta} \quad (17)$$

To determine the increase in crack widths Δw_{k2} according to (16), Table 1 also compares the values of the mean degree of relaxation $\overline{\Delta R_{ax}}$ (s_{rml}/L) determined with the assumption of the relative crack spacing defined by Eq. (17). The obtained values $\overline{\Delta R_{ax}}$ (s_{rml}/L) as a function of h_1/H and α_D are several times greater than $\overline{\Delta R_{ax}}$ ($0.5L/L$). However, a much shorter range of the relaxation zone means that the values of Δw_{k2} at the same ΔT will be much smaller relative to w_{k1} .

The relative spacing of the cracks s_{rml}/H is summarized in Table 2. The smallest values refer to very high walls—that is, those where the relative height of the crack initial level is small ($h_1 = 0.05H$). The effective degree of relaxation after cracking at this level is the smallest due to the relative closeness to the horizontal restrained edge. Considering non-reinforced walls ($\alpha_D = 0$), for example, for the values of $h_1 = 0.05H$ and $0.4H$, the crack spacing is $0.537H$ and $2H$, respectively. As the degree of reinforcement increases (that is, with an increased stiffness in the crack), the relative value of the crack spacing decreases and the influence of the h_1/H height on the crack spacing becomes smaller. For $\alpha_D = 2.5$ as well as $0.05H$ and $0.4H$, the s_{rml} values of $0.085H$ and $0.102H$ were obtained, respectively. This model assumes that the present state is the distribution of the basic first-order cracks (s_{rml}), and further imposed loads will result in increasing crack widths and the formation of new, narrower second-order cracks. Water-tightness should be ensured at the level of the first-order cracks. It should be added that the crack spacing calculated in this way (Table 2) cannot be smaller than the one defined by Eq. (7.11⁹).

When determining the value of w_{k1} , very high walls $h_1/H = 0.05$ are definitely the most favorable, as an increase in the h_1/H ratio contributes to greater relaxation at this level.

For determining Δw_{k2} , a smaller crack spacing for smaller values of h_1/H contributes to a more averaged relaxation of concrete between the cracks. Similar to the mean value of the wall relaxation $\overline{\Delta R_{ax}}$ (0.5 L/L), greater reinforcement results in smaller values of the average wall relaxation $\overline{\Delta R_{ax}}$ (s_{rml}/L), and this effect is even more visible when the value of h_1/H increases.

Criterion for formation of second-order cracks

Based on the adopted surface of steel and the formula describing the minimum reinforcement surface (7.1),⁹ a stress limit (σ_{sl}^{lim}) in this reinforcement was determined that, when exceeded, would lead to the formation of second-order cracks

$$\sigma_{sl}^{lim} = k_c \cdot k \cdot f_{ct,eff}(t) \cdot A_{ct}/A_s \quad (18)$$

In the next step, by substituting σ_{sl}^{lim} into Eq. (2),²⁶ a crack width limit (w_{k2}^{lim}) was obtained—that is, a value characteristic of the state just before the occurrence of second-order cracks. Then, from Eq. (16), it is possible to determine the strain $\varepsilon_{free2}^{lim}$ limits that ΔT_2 results from

$$\varepsilon_{free2}^{lim} = \frac{w_{k2}^{lim} - w_{k1}}{s_{rml} \cdot \overline{\Delta R_{ax}} \left(\frac{-s_{rml}}{2L}; \frac{s_{rml}}{2L} \right) \cdot k_\phi} + \frac{\Delta R_{ax} \cdot f_{ct,eff}}{E_{cm}(t_{cr2})} \quad (19)$$

in which the validity of using the $k\phi$ coefficient results only from the large time interval between crack initiation (t_{cr}) and the initiation of first-order cracks with a stabilized spacing (t_1).

Increase in crack width from further temperature changes

When ΔT_2 is exceeded, the spacing of the cracks will decrease to s_r^{max} . The excess imposed load, due to temperature change and shrinkage, will contribute to the formation of new cracks in the tie model (Eq. (M.1)⁴) and to the widening of existing cracks. Due to the reduction in the crack spacing, the difference between the average strain of steel and concrete increases at the distance s_r^{max} (where s_r^{max} is described after EN 1992-1-1⁹) according to the following expression

$$\begin{aligned} \Delta(\varepsilon_{sm} - \varepsilon_{cm})_{II}' &= 0.5 \cdot \alpha_e(t_2 > t_1) \cdot k_c \cdot k \cdot f_{ct,eff}(t_2 > t_1) \\ &\cdot (1 + 1/\alpha_e(t_2 > t_1) \cdot \rho)/E_s - 0.5 \cdot \alpha_e(t_1) \cdot k_c \\ &\cdot k \cdot f_{ct,eff}(t_1) \cdot (1 + 1/\alpha_e(t_1) \cdot \rho)/E_s \end{aligned} \quad (20)$$

After additional thermal strains, the width increase of first-order cracks calculated in accordance with the tie model (EN 1992-1-1⁹) can be defined as follows

$$\Delta w_{k3}' = s_r^{max} \cdot \Delta(\varepsilon_{sm} - \varepsilon_{cm})_{II}' \quad (21)$$

in which s_r^{max} is the maximum spacing between the second-order cracks, including the self-equilibrating stresses in the

k_2 coefficient resulting from a non-uniform temperature field, internal restraints, and poor bond conditions; that is, $\eta_1 = 0.7$.

Shrinkage strain

The increment of the difference in the strains between steel and concrete resulting from shrinkage in the hardened concrete can be calculated from the following expression

$$\begin{aligned} \Delta(\varepsilon_{sm} - \varepsilon_{cm})_{II}'' &= 0.5 \cdot \alpha_{e28} \cdot k_c \cdot k \cdot f_{ct,eff28} \cdot (1 + 1/\alpha_{e28} \cdot \rho)/E_s \\ &- 0.5 \cdot \alpha_e(t_2) \cdot k_c \cdot k \cdot f_{ct,eff}(t_2) \cdot (1 + 1/\alpha_e(t_2) \cdot \rho)/E_s \end{aligned} \quad (22)$$

At this time, the crack spacing is further reduced by surface tensile stresses from shrinkage. This fact is taken into consideration in the expression for s_r^{max} by the coefficient $k_2 = (\varepsilon_1 + \varepsilon_2)/2\varepsilon_1$, in which ε_1 is a restrained strain on the wall surface, and ε_2 is a restrained strain in the wall axis or, if justified, in the concrete layer located between the axis and the wall surface. Flaga³⁴ specified the approximate thickness of zone b_1 subjected to tensile stress as a result of internal restraints. The value of b_1 is adopted in the calculations not only to determine the area requiring reinforcement but also to determine the resultant of these stresses,³⁴ and this value can be considered in the k_2 coefficient. A smaller value of b_1 relative to the wall thickness should result in a smaller crack spacing. Therefore, in the case of reinforced members, it is suggested that $k_2 = [(\varepsilon_1 + \varepsilon_2)/2\varepsilon_1] \cdot (b_1/0.5h)$. In the case of non-reinforced members or for those in which the reinforcement spacing exceeds $5 \cdot (c + \phi/2)$, it can be predetermined after Eq. (7.14)⁹ that $s_r^{max} = 1.3(h - x)$, that is, $1.3b_1$.

The increase in first-order crack width resulting from shrinkage according to the tie model (EN 1992-1-1⁹) can be defined as follows

$$\Delta w_{k3s}'' = s_r^{max} \cdot \Delta(\varepsilon_{sm} - \varepsilon_{cm})_{II}'' \quad (23)$$

External loads

As in the tie model, the increment of the difference in the average strains from external loads (for example, liquid pressure in the tank during water-tightness test or operation) between steel and concrete takes the following form

$$\Delta(\varepsilon_{sm} - \varepsilon_{cm})_{III}'' = \Delta\varepsilon_{smII} - \Delta\varepsilon_{cmII} \quad (24)$$

where

$$\Delta\varepsilon_{smII} = \frac{\sigma_{sII}}{E_s} - \left(\frac{k_t \cdot f_{ct,eff}(28 \text{ days})}{E_s \cdot \rho_{p,eff}} - \frac{k_t \cdot f_{ct,eff}(t_3)}{E_s \cdot \rho_{p,eff}} \right) \quad (25)$$

$$\Delta\varepsilon_{cmII} = \frac{k_t \cdot f_{ct,eff}(28 \text{ days})}{E_{cm}(28 \text{ days})} - \frac{k_t \cdot f_{ct,eff}(t_3)}{E_{cm}(t_3)} \quad (26)$$

Thus, increase in the first-order crack width is defined as follows

$$\Delta w_{k3Z}'' = s_r^{max} \cdot \Delta(\epsilon_{sm} - \epsilon_{cm})_{IIZ}'' \quad (27)$$

The final width of the first crack is calculated from the following expression

$$w_{k3} = w_{k1} + \Delta w_{k2} + \Delta w'_{k3} + \Delta w''_{k3S} + \Delta w''_{k3Z} \quad (28)$$

If $s_{rml} \leq s_{r,max}$, then the calculations should be performed according to the tie model, by leaving out Δw_{k2} .

SUMMARY AND CONCLUSIONS

Based on the results of this analytical investigation of semi-massive RC tank wall cracking, the following conclusions are drawn:

1. In the calculation of the crack width, it is necessary to distinguish between first-order and second-order cracks, consider the stages of crack formation and the increase in their width with subsequent loading stages.

2. The crack widths formed from wall cooling during concrete curing do not depend directly on the degree of restraint. The basic factor determining the crack width is the mean value of the degree of wall relaxation that depends on the degree of restraint, crack initial level h_1/H , location of external restraints and stiffness D_{11} determining the cracked section stiffness—that is, the diameter of reinforcing bars ϕ and the degree of reinforcement ρ .

3. Similarly, the first-order crack spacing depends not only on the degree of reinforcement but also on the distribution of the wall relaxation degree.

4. First-order cracks, which occur the earliest, play an essential role in meeting the permissible crack width. Consequently, the proposed model includes the stages of crack formation and the increase in their widths with subsequent stages of loading.

5. A high degree of restraint may not always form the basis for a large relaxation—that is, a crack with a large width.

6. An increase in the first-order crack width during the formation of second-order cracks depends on the increments of loads (stresses in steel), changing values of concrete mechanical properties, and the resulting increase in crack widths depending on the increment of the difference in average strain between steel and concrete.

AUTHOR BIOS

Mariusz Zych is an Academic at Cracow University of Technology, Krakow, Poland. He received his doctorate of technical sciences at Cracow University of Technology and earned a postdoctoral degree. His research interests include watertightness and durability of semi-massive reinforced concrete tank walls, early-age cracking, and design and strengthening of reinforced concrete and prestressed tanks for the storage of liquids.

NOTATION

a	= half of crack spacing length
c	= cover to longitudinal reinforcement
	= normal stiffness modulus
E_{cm}	= secant modulus of elasticity of concrete
	= modulus of elasticity of reinforcing steel (200 GPa [2.9 Mpsi])
$f_{ct,eff}$	= mean value of tensile strength of concrete effective at time when cracks may be expected to occur: $f_{ct,eff} = f_{cm}(t, T)$
f_{cm}	= mean value of axial tensile strength of concrete
H	= wall height
h_1	= height of critical section where first cracking occurs

k	= coefficient accounting for non-uniform self-equilibrating stresses leading to reduction of restraint forces
k_1	= coefficient accounting for bond properties of bonded reinforcement
k_2	= coefficient accounting for strain distribution
k_b	= distributed bond-slip stiffness along reinforcement bar defined as ratio between bond stress and slip
k_c	= coefficient accounting for stress distribution within section immediately prior to second-order cracking
k_t	= coefficient depending on duration of load
k_ϕ	= coefficient accounting for concrete creep (according to CIRIA, ³⁵ $k_\phi = 0.65$)
L	= length of segment wall
$R_{ax}(\alpha, D)$	= degree of restraint in discrete cracks as function of their stiffness
R_{ax}^{cr}	= restraint factor for cracked element
R_{ax}^{ncr}	= restraint factor for noncracked element
$R_{ax}^{ucr}(s_{rml})$	= effective degree of restraint at s_{rml} distance from first crack
t_1	= time at which cracks are formed in s_{rml} spacing
α_D	= ratio of stiffness in discrete crack D_{11} to modulus of wall elasticity E_{cm}
α_e	= ratio E_s/E_{cm}
α_T	= thermal expansion coefficient of concrete
$\frac{\Delta R_{ax}}{\Delta R_{ax}}$	= degree of relaxation
$\frac{\Delta R_{ax}}{\Delta R_{ax}}$	= mean degree of relaxation
$\frac{\Delta R_{ax}}{\Delta R_{ax}}(0.5L/L)$	= mean degree of relaxation for crack spacing of $0.5L$
$\frac{\Delta R_{ax}}{\Delta R_{ax}}(s_{rml}/L)$	= mean degree of relaxation for s_{rml} crack spacing
ΔT	= concrete temperature change
ΔT_{cr}	= temperature change resulting in formation of first crack at time t_{cr}
$\Delta \epsilon_{cmII}$	= increment of average concrete strain occurring between cracks caused by external loads
$\Delta \epsilon_{smII}$	= increment of average steel strain occurring between cracks caused by external loads
ϵ_{cm}	= mean strain in concrete between cracks
ϵ_{ctu}	= tensile strain capacity of concrete
ϵ_{free}	= imposed strain
ϵ_{sm}	= mean strain in reinforcement
ϕ	= bar diameter
η_1	= coefficient related to bond condition quality
ρ	= degree of reinforcement
$\rho_{p,eff}$	= effective degree of reinforcement = $A_s/A_{c,eff}$ ($A_{c,eff}$ as defined in EN 1992-1-1 ⁹)
σ_s	= stress in tension reinforcement after cracking
σ_{sII}	= additional stress in reinforced steel caused by external loads

REFERENCES

1. Stoffers, H., "Cracking Due to Shrinkage and Temperature Variation in Walls," third edition, Delft University of Technology and I.B.B.C., Delft, the Netherlands, V. 23, No. 3, 1978, 68 pp.
2. ACI Committee 207, "Report on Thermal and Volume Change Effects on Cracking of Mass Concrete (ACI 207.2R-07)," American Concrete Institute, Farmington Hills, MI, 2007, 28 pp.
3. BS, "Design of Concrete Structures for Retaining Aqueous Liquids (8007)," British Standards Institution, London, UK, 1987, 28 pp.
4. CEN, "Eurocode 2 – Design of Concrete Structures — Part 3: Liquid Retaining and Containment Structures (EN 1992-3)," European Committee for Standardization, Brussels, Belgium, 2006, 23 pp.
5. NZS, "Design of Concrete Structures for the Storage of Liquids (3106:2009)," Standards New Zealand, Wellington, New Zealand, 2009, 81 pp.
6. Iványi, G., "Bemerkungen zu Mindestbewehrung in Wänden," *Beton- und Stahlbetonbau*, V. 90, No. 11, 1995, pp. 283-289. doi: 10.1002/best.199500460
7. Rostásy, F. S., and Henning, W., "Zwang in Stahlbetonwänden auf Fundamenten," *Beton- und Stahlbetonbau*, V. 84, No. 8-9, 1989, pp. 208-214 and 232-237.
8. Zych, M., "The Influence of Ambient Temperature on RC Tank Walls Watertightness in Research and Theory," *Periodica Polytechnica. Civil Engineering*, V. 59, No. 3, 2015, pp. 267-278. doi: 10.3311/PPci.7728
9. CEN, "Eurocode 2 - Design of Concrete Structures — Part 1-1: General Rules and Rules for Buildings (EN 1992-1-1)," European Committee for Standardization, Brussels, Belgium, 2004, 205 pp.

10. Buffo-Lacarière, L.; Sellier, A.; Turatsinze, A.; and Escadeillas, G., "Finite Element Modelling of Hardening Concrete, Application to the Prediction of Early Age Cracking for Massive Reinforced Structures," *Materials and Structures*, V. 44, No. 10, 2011, pp. 1821-1835. doi: 10.1617/s11527-011-9740-y
11. Klemczak, B., and Knoppik-Wróbel, A., "Degree of Restraint Concept in Analysis of Early-Age Stresses in Concrete Walls," *Engineering Structures*, V. 102, No. 11, 2015, pp. 369-386.
12. Liu, X.; Yuan, Y.; and Su, Q., "Sensitivity Analysis of the Early-Age Cracking Risk in an Immersed Tunnel," *Structural Concrete*, V. 15, No. 2, 2014, pp. 179-190. doi: 10.1002/suco.201300064
13. Wu, S.; Huang, D.; Lin, F.-B.; Zhao, H.; and Wang, P., "Estimation of Cracking Risk of Concrete at Early Age Based on Thermal Stress Analysis," *Journal of Thermal Analysis and Calorimetry*, V. 105, No. 1, 2011, pp. 171-186. doi: 10.1007/s10973-011-1512-y
14. Kheder, G. F., "A New Look at the Control of Volume Changes Cracking Base Restrained Concrete Walls," *ACI Structural Journal*, V. 94, No. 3, May-June 1997, pp. 262-271.
15. Kheder, G. F.; Al-Rawi, R. S.; and Al-Dhahi, J. K., "A Study of the Behavior of Volume Change Cracking in Base Restrained Concrete Walls," *Materials and Structures*, V. 27, No. 7, 1994, pp. 383-392. doi: 10.1007/BF02473441
16. Al Rhawi, R. S., and Kheder, G. F., "Control of Cracking Due to Volume Change in Base-Restrained Concrete Members," *ACI Structural Journal*, V. 87, No. 4, July-Aug. 1990, pp. 397-405.
17. Scott, R. H., and Gill, P., "Short Term Distribution of Strain and Bond Stress Along Tension Reinforcement," *Structural Engineering*, V. 65B, No. 2, 1987, pp. 39-43.
18. Beeby, A. W., and Forth, J. P., "Control of Cracking Walls Restrained Along Their Base against Early Thermal Movements," *Proceedings of the 6th International Congress on Global Construction, Ultimate Concrete Opportunities*, Thomas Telford, London, UK, 2005, pp. 123-132.
19. Beeby, A. W., and Narayanan, R. S., "Designers' Guide to EN 1992-1-1 and EN 1992-1-2 Eurocode 2: Design of Concrete Structures. General Rules and Rules for Buildings and Structural Fire Design," Thomas Telford, London, UK, 2005, 242 pp.
20. Anson, M., and Rowlinson, P. M., "Early-Age Strain and Temperature Measurements in Concrete Tank Walls," *Magazine of Concrete Research*, V. 40, No. 145, 1988, pp. 216-226. doi: 10.1680/mac.1988.40.145.216
21. Anson, M., and Rowlinson, P. M., "Field Measurements for Early-Age Strains in Concrete," *Magazine of Concrete Research*, V. 42, No. 153, 1990, pp. 203-212. doi: 10.1680/mac.1990.42.153.203
22. Pettersson, D., and Thelandersson, S., "Crack Development in Concrete Structures Due to Imposed Strains. Part I: Modelling," *Materials and Structures*, V. 34, No. 1, 2001, pp. 7-13. doi: 10.1007/BF02482194
23. Pettersson, D.; Alemo, J.; and Thelandersson, S., "Influence on Crack Development in Concrete Structures from Imposed Strains and Varying Boundary Conditions," *Construction and Building Materials*, V. 16, No. 4, 2002, pp. 207-213. doi: 10.1016/S0950-0618(02)00007-7
24. Zych, M., "Degree of External Restraint of Wall Segments in Semi-Massive Reinforced Concrete Tanks: Part II: Rectangular and Cylindrical Segments," *Structural Concrete: Journal of the fib*, V. 19, No. 3, 2018, pp. 829-838. doi: 10.1002/suco.201700037
25. Eurocode 2, "Bemessung und Konstruktion von Stahlbeton- und Spannbetontragwerken – Teil 1-1: Allgemeine Bemessungsregeln und Regeln für den Hochbau (DIN EN 1992-1-1/NA2011-01)," Nationaler Anhang, Berlin, Germany, 2011.
26. Zych, M., "Degree of External Restraint of Wall Segments in Semi-Massive Reinforced Concrete Tanks: Part I Rectangular Segments," *Structural Concrete: Journal of the fib*, V. 19, No. 3, 2018, pp. 820-828. doi: 10.1002/suco.201700036
27. Zych, M., "Thermal Cracking of the Cylindrical Tank under Construction. II: Early Age Cracking," *Journal of Performance of Constructed Facilities*, ASCE, V. 29, No. 4, 2015, pp. 1-10. doi: 10.1061/(ASCE)CF.1943-5509.0000577
28. Zych, M., "Case Study of Concrete Mechanical Properties Development Based on Heat Temperature Measurements," *Cement, Wapno, Beton*, No. 6, 2015, pp. 383-392.
29. Seruga, A., and Zych, M., "Research of Concrete Creep at Early Age under Compressive and Tensile Stresses," *Cement, Wapno, Beton*, No. 2, 2016, pp. 65-77.
30. Seruga, A., and Zych, M., "Thermal Cracking of the Cylindrical Tank under Construction. I: Case Study," *Journal of Performance of Constructed Facilities*, ASCE, V. 29, No. 4, 2015, pp. 1-9. doi: 10.1061/(ASCE)CF.1943-5509.0000581
31. Zych, M., "Analysis of RC Tank's Walls during Early Hardening Period of Concrete, in Aspect of Water-Tightness," doctoral thesis, Division of Structural Engineering, Cracow University of Technology, Krakow, Poland, 2011, 246 pp.
32. Ouzaa, K., and Benmansour, M. B., "Cracks in Base-Restrained Plain and Reinforced Concrete Walls," *Turkish Journal of Engineering and Environmental Sciences*, V. 34, No. 3, 2010, pp. 215-230.
33. Seruga, A.; Szydłowski, R.; and Zych, M., "The Evaluation of Sequential Process of Cracking of Wall Segments in Monolithic Cylindrical Reinforced Concrete Tanks," *Technical Transactions*, Civil Engineering, No. 1-B, 2008, pp. 135-163.
34. Flaga, K., "Shrinkage Stresses and Surface Reinforcement in Concrete Structures," Monograph 391, Cracow University of Technology, Cracow, Poland, 2011.
35. Bamforth, P. B., "Early-Age Thermal Crack Control in Concrete," CIRIA C660, London, UK, 2007.